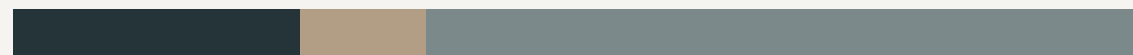




Inside A Collaborative Cell: Calibration, Perception And Safety Requirements



October 30, 2025

Daniela Rato
PhD Mechanical Engineering
Supervised by Prof. Miguel Oliveira, Prof. Vítor Santos and Prof. Angel Sappa

Motivation

- Collaborative robots are moving into dynamic, human-shared environments.
- Mechanical safety is not enough → perception-driven cobots are needed.
- Accurate perception requires multiple sensors from different modalities → robust extrinsic calibration is needed.
- Robust perception requires:
 - **Accurate extrinsic calibration** across heterogeneous sensors;
 - **Reliable 3D human pose estimation** under occlusion and real-world variability.



Research Objectives

- ▶ To investigate how the existing calibration framework can be applied and **extended** for use in **robotic collaborative cell** scenarios.
 - ▶ Adapt and enhance Atomics Transformation Optimization Method for robotic cells, including **RGB-D** and hand-eye **RGB-D** calibration.
 - ▶ Ensure **modularity** and **integration** into robot operating environments.
- ▶ To design and implement a **3D human pose estimation** framework tailored to **collaborative robotics**.
 - ▶ **Multi-camera RGB** approach tailored for collaborative robots.
 - ▶ Optimised for **robustness under occlusion** and real-world deployment.

Research Questions

- ▶ How can calibration algorithms be designed to support heterogeneous, **multi-modal sensor setups**, including both **fixed and mobile configurations**, while reducing reliance on manual procedures and maintaining spatial accuracy?
- ▶ What optimisation strategy enables consistent and **accurate extrinsic calibration in dynamic environments** where sensor positions or orientations may vary over time?
- ▶ How can **3D human pose estimation** systems based solely on RGB imagery be configured to offer sufficient accuracy, **robustness to occlusion**, and **computational efficiency** for integration into collaborative robotic environments?

Research Questions

- ▶ How can calibration algorithms be designed to support heterogeneous, **multi-modal sensor setups**, including both **fixed and mobile configurations**, while reducing reliance on manual procedures and maintaining spatial accuracy?
- ▶ What optimisation strategy enables consistent and **accurate extrinsic calibration in dynamic environments** where sensor positions or orientations may vary over time?
- ▶ How can 3D human pose estimation systems based solely on RGB imagery be configured to offer sufficient **accuracy, robustness to occlusion, and computational efficiency** for integration into collaborative robotic environments?

Hypothesis

robust calibration

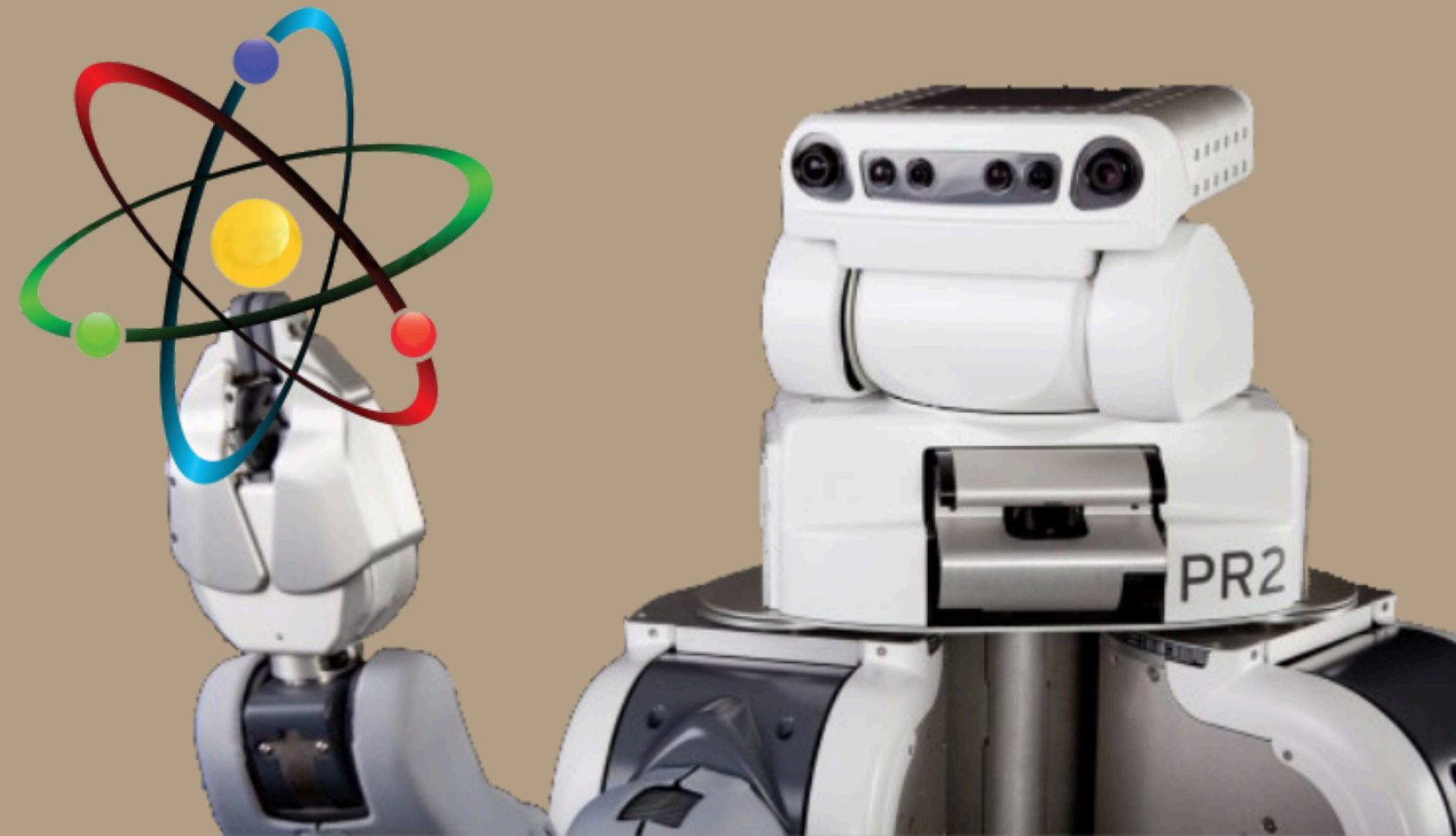
+

accurate pose estimation

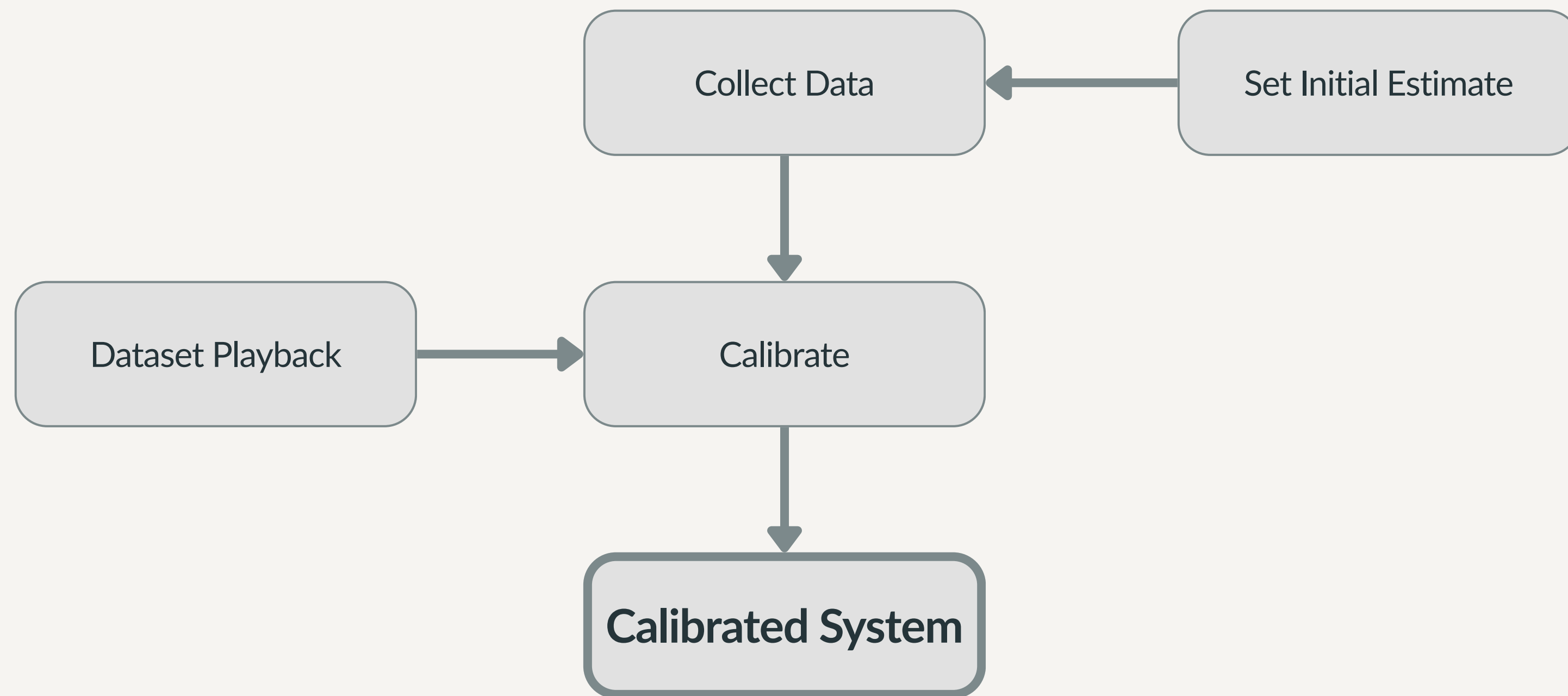
=

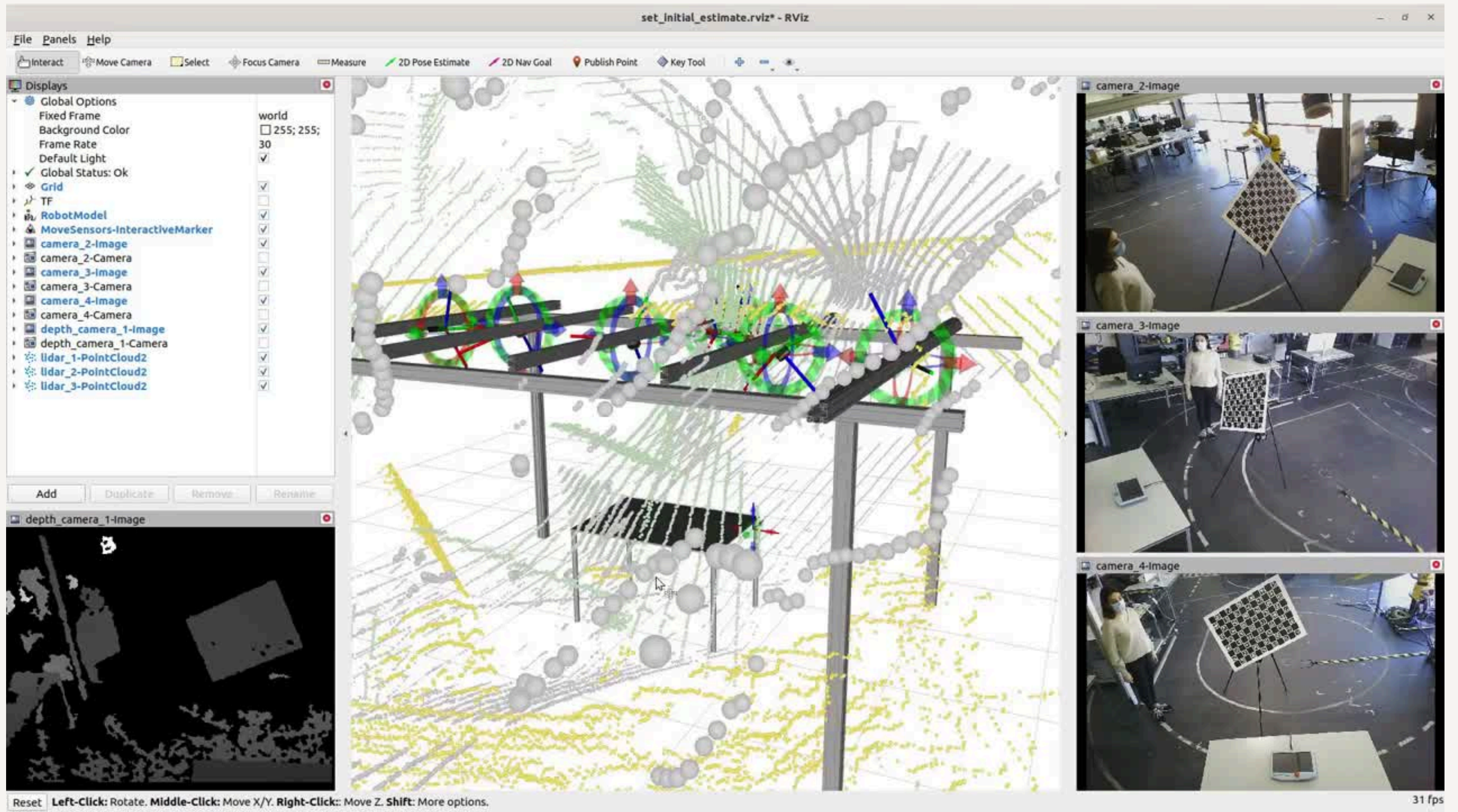
a safer human-robot collaboration

ATOM: Atomic Transformations Optimization Method



ATOM Framework

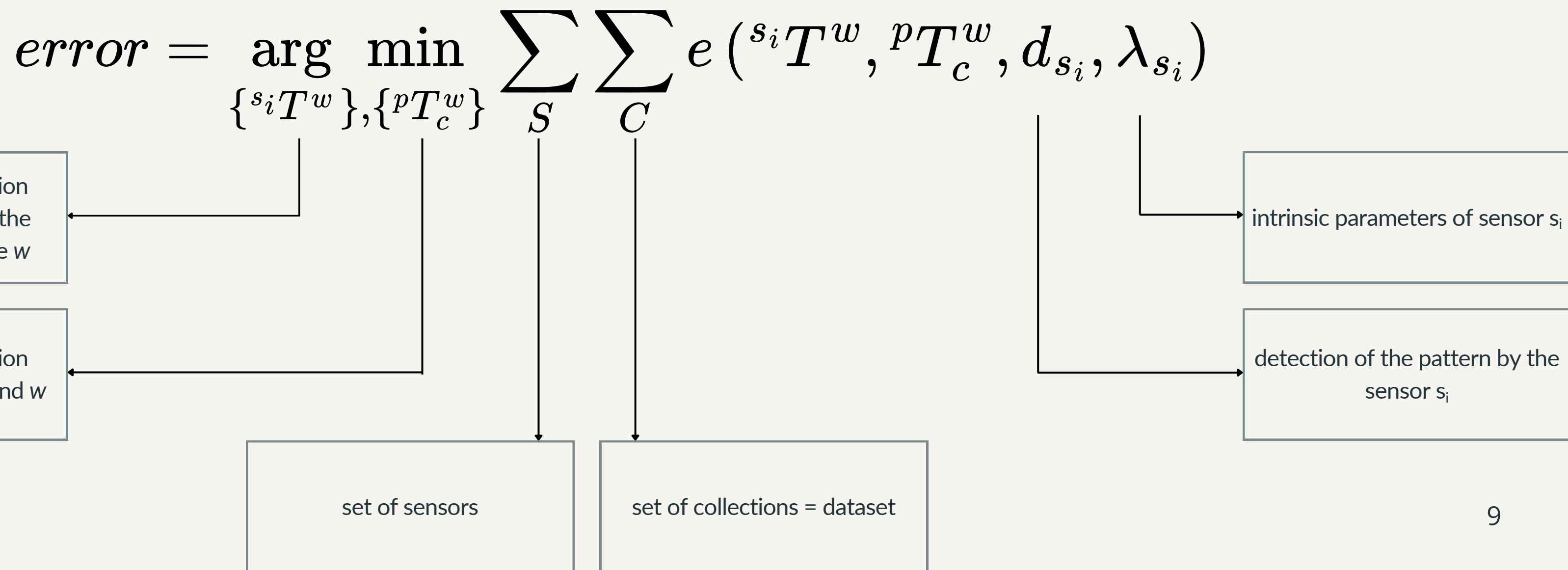




speed: 4x

Calibration Formulation

Sensor to Pattern Approach



Depth Modality Extension

Orthogonal Error

$$e_{o[c,s]} = \left[({}^s T_c^p)^{-1} \cdot X_{[c,s]} \right]_z$$

estimated transformation
between the sensor s and the
pattern p for a collection c

detected pattern points for a
collection c and sensor s

Longitudinal Error

$$e_{l_{[c,s,b]}} = \min_{q \in Q} \left(\left\| \left[q - ({}^s T_c^p)^{-1} \cdot X_{[c,s,b]} \right]_{xy} \right\|_F^2 \right)$$

Depth Modality Extension

Orthogonal Error

$$e_{o_{[c,s]}} = \left[({}^sT_c^p)^{-1} \cdot X_{[c,s]} \right]_z$$

Longitudinal Error

$$e_{l_{[c,s,b]}} = \min_{q \in Q} \left(\left\| \left[q - ({}^sT_c^p)^{-1} \cdot X_{[c,s,b]} \right]_{xy} \right\|_F^2 \right)$$

sampled pattern border point

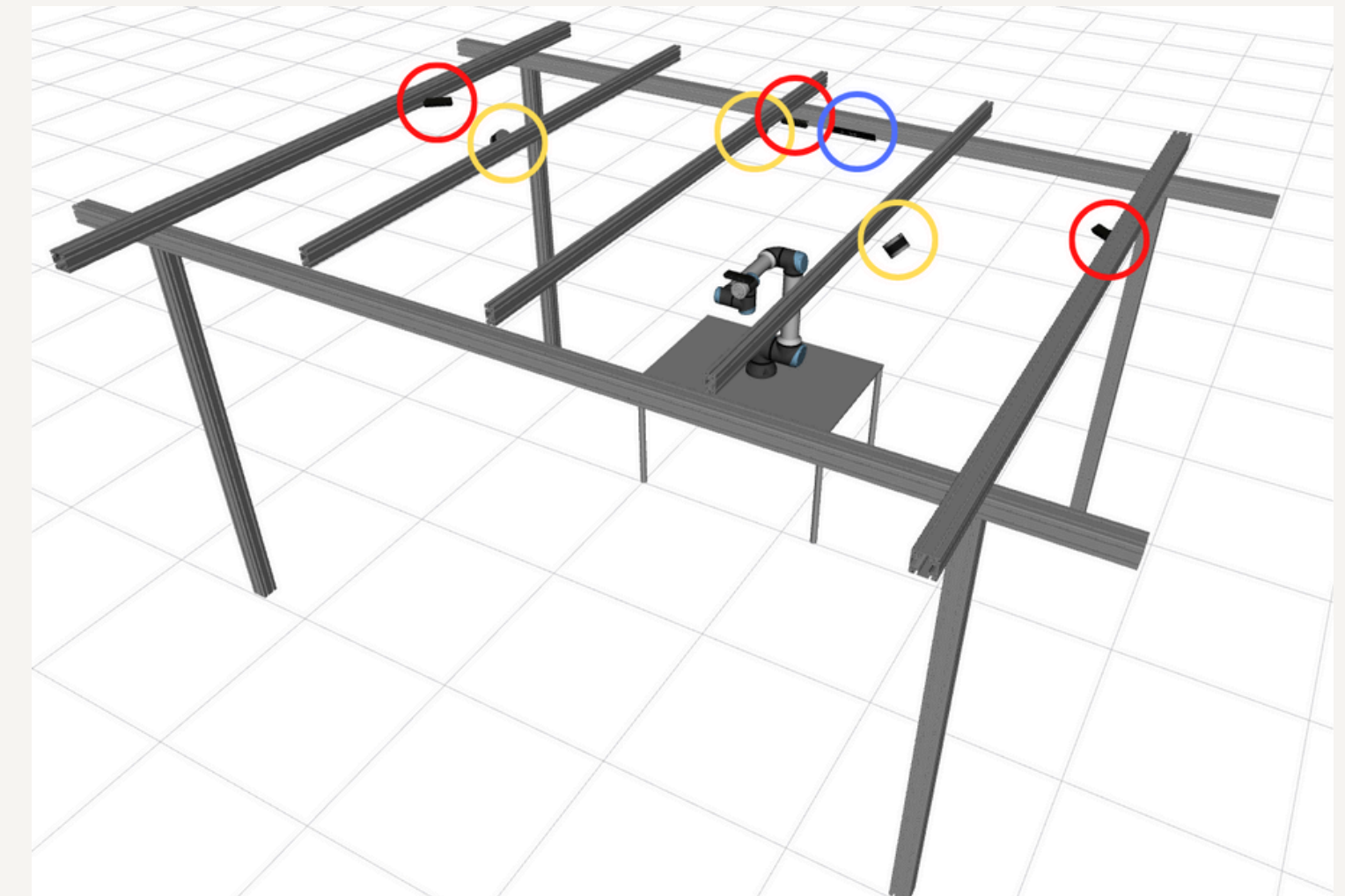
detected boundary points for a collection c and sensor s

Setup - Collaborative Cell

Real World

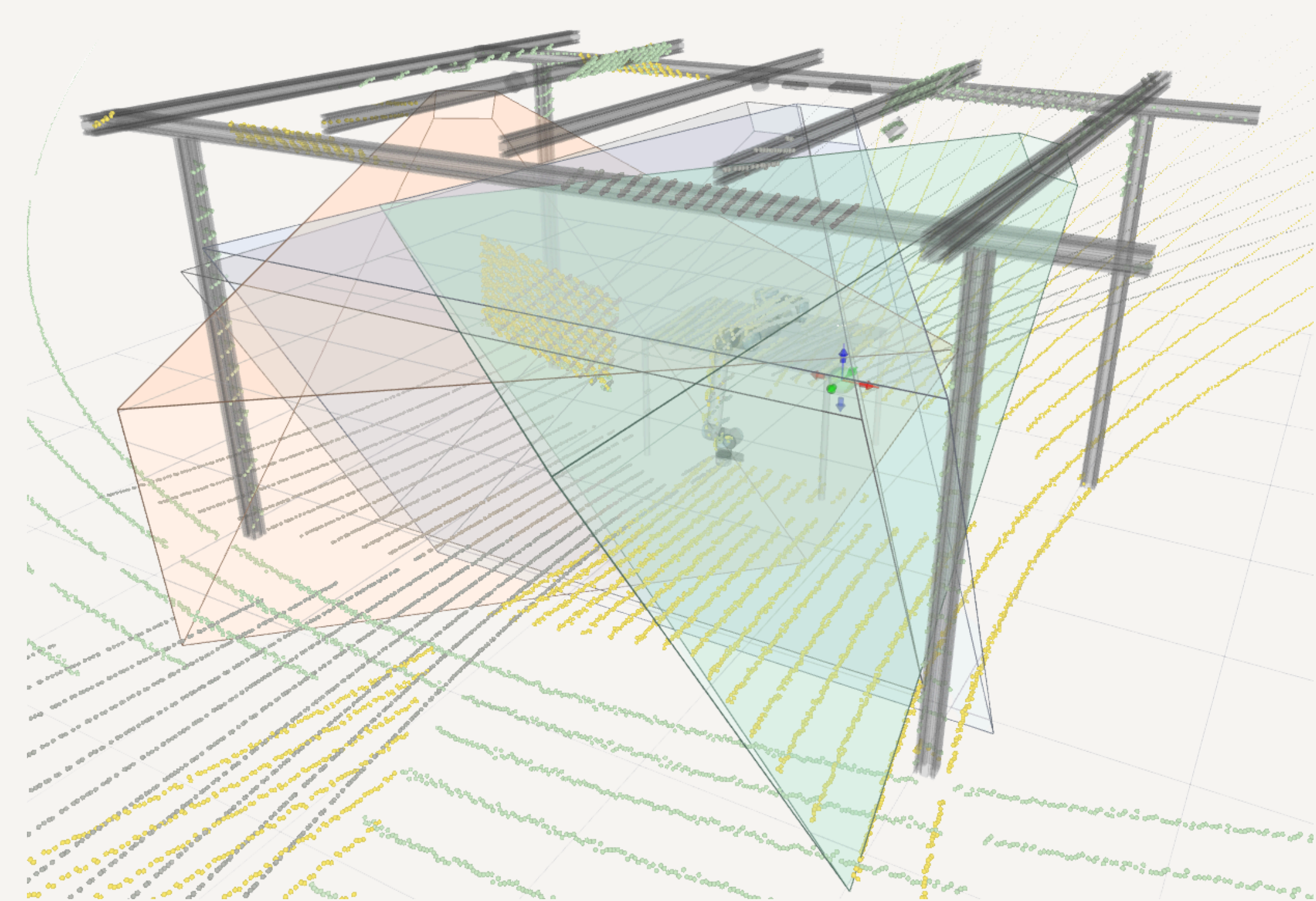


Simulation



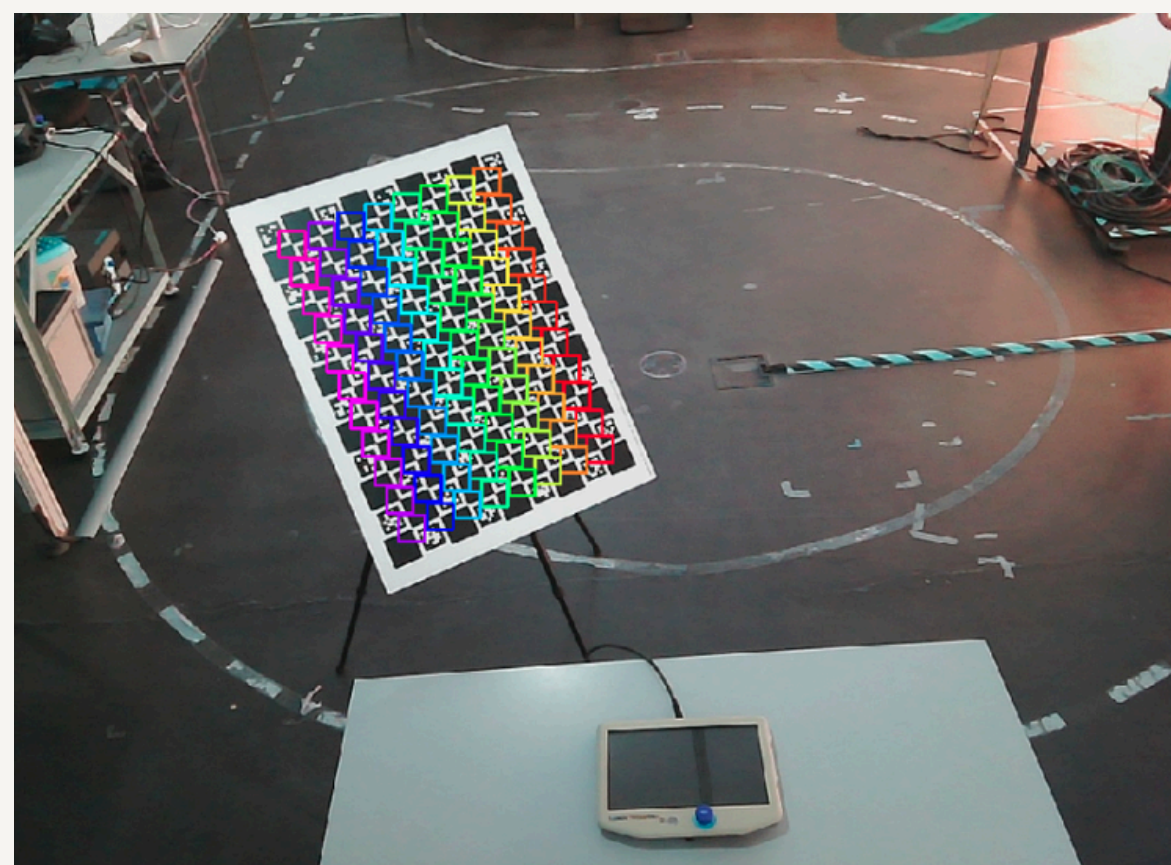
Red - RGB-D; Yellow - LiDAR; Blue - RGB

Fields-of-view

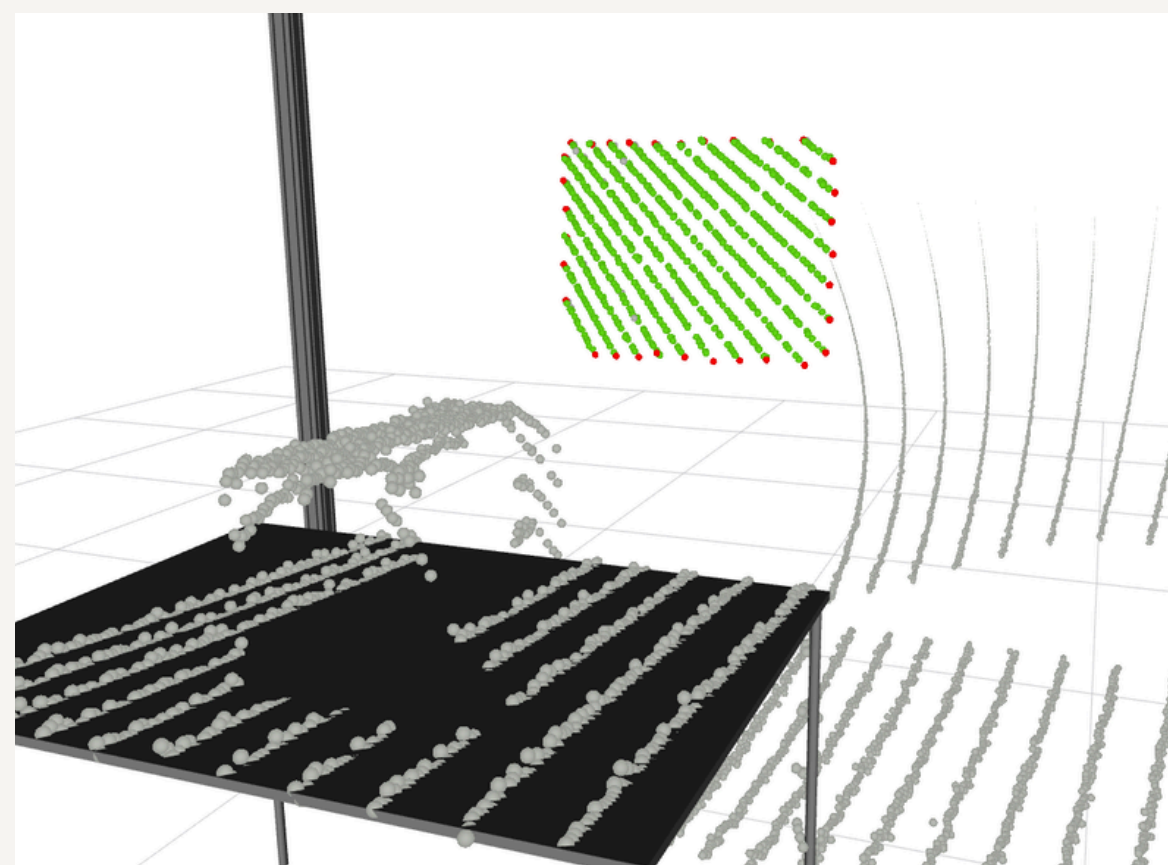


Example of labelled data

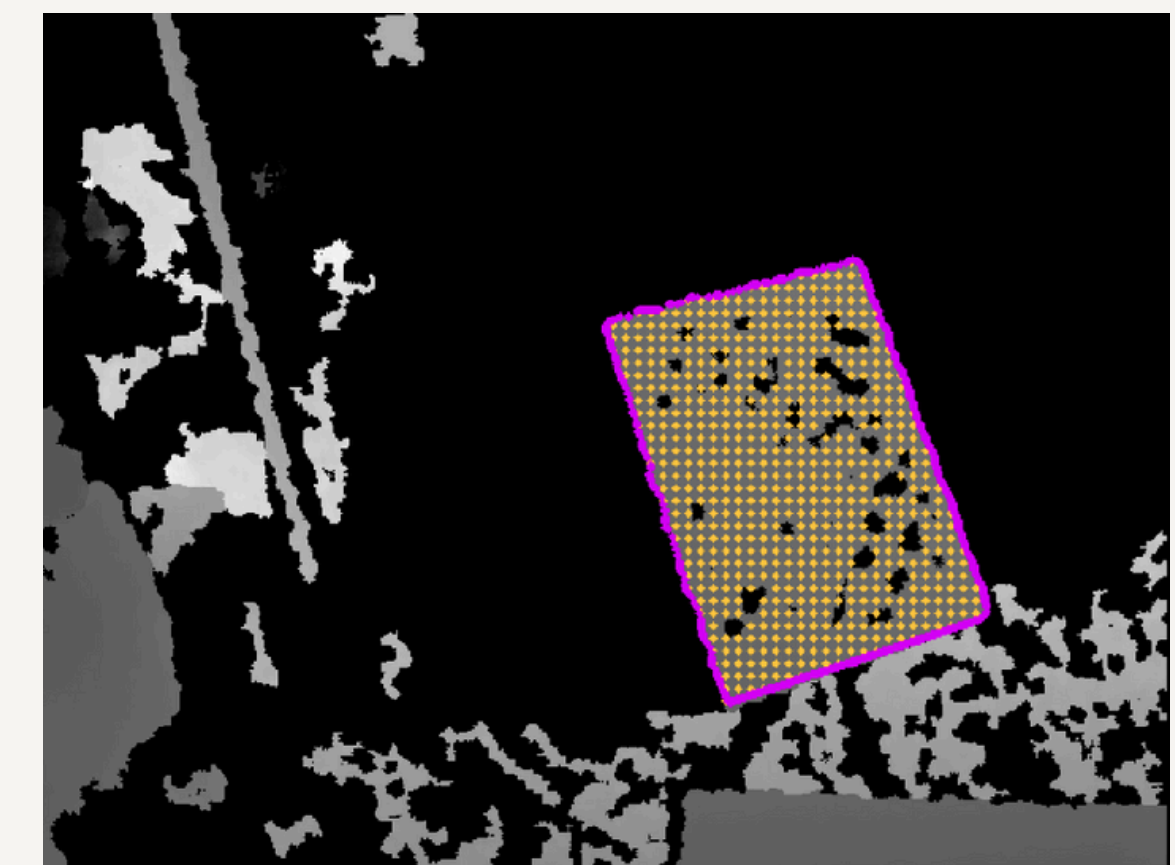
RGB



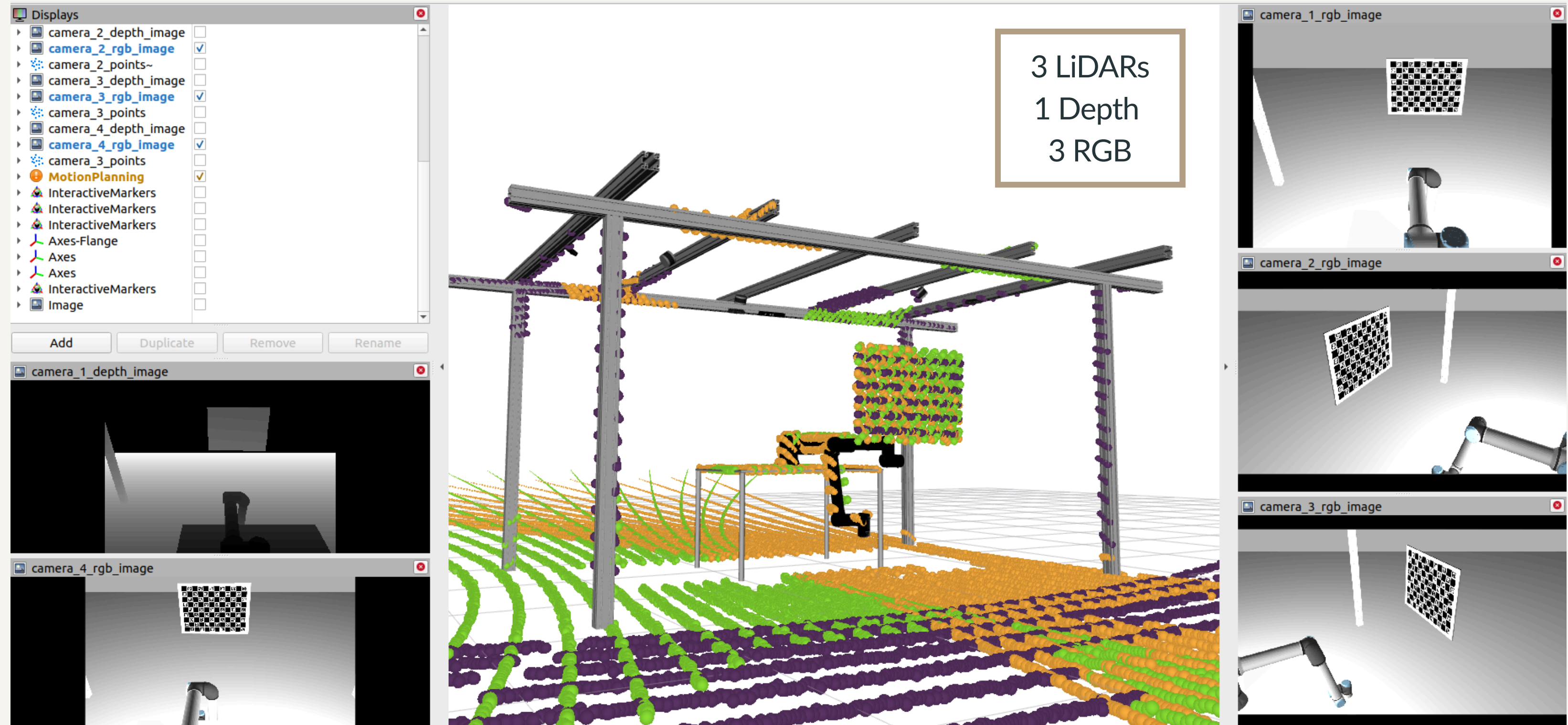
LiDAR



Depth



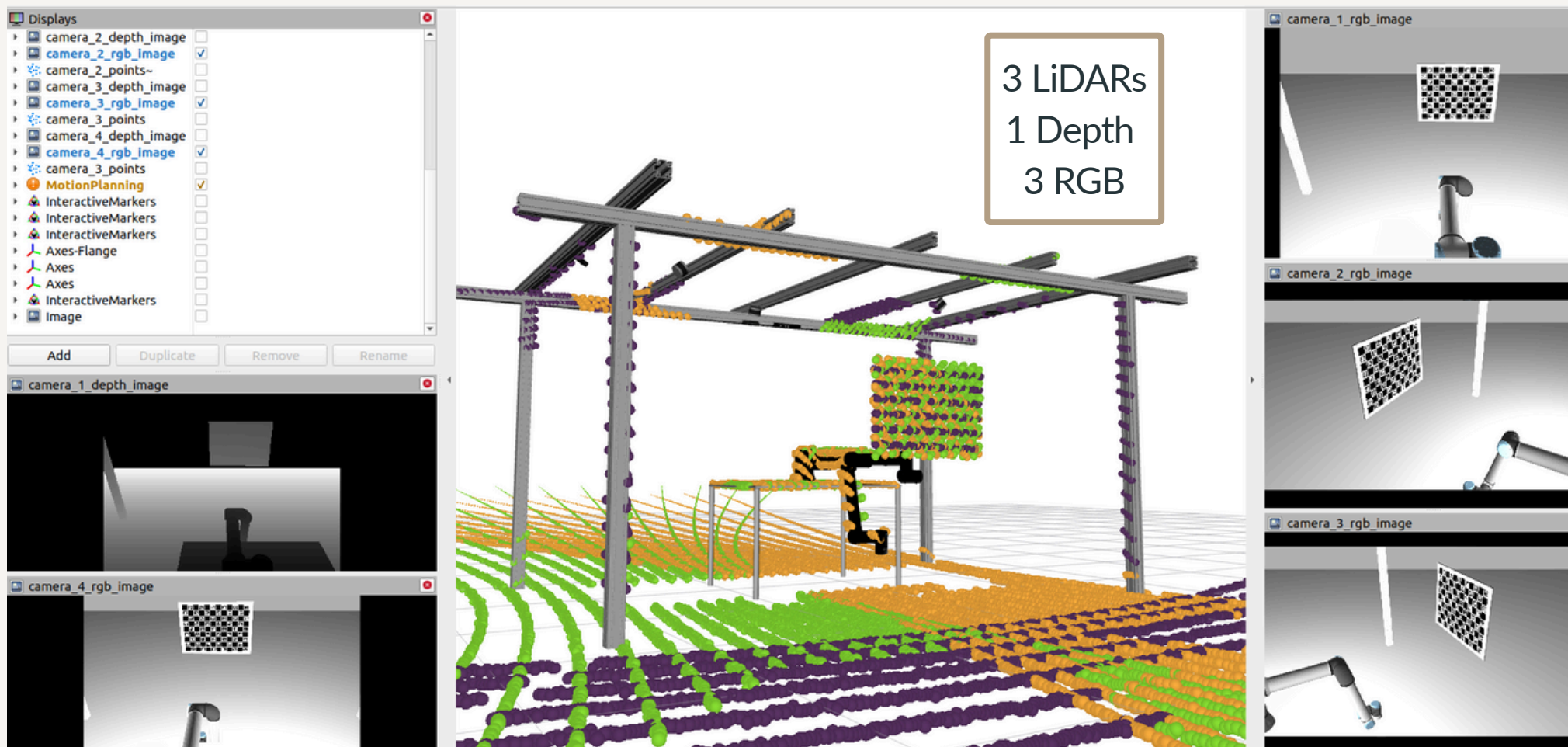
Case Study 1



Case Study 1

Descriptions of the datasets used in this case study.

Type of data	Dataset	# collections	# partials	# complete
Simulation	train dataset	23	35	5
	test dataset	17	26	4
Real data	train dataset	29	61	6
	test dataset	14	29	4



Case Study 1

Comparative results

Average RGB-RGB root mean square reprojection errors in pixels.

Method	Simulation	Real
Ours	0.6	1.3
OpenCV	0.6	1.8
Kalibr	1.3	0.8

Average LiDAR-LiDAR root mean square reprojection errors in millimetres.

Method	Simulation	Real
Ours	33.0	53.6
ICP Initial Avg	249.4	173.4
ICP Initial Best	36.5	162.8
ICP Aligned Avg	33.9	53.3
ICP Aligned Best	91.7	109.9

Average LiDAR-depth root mean square reprojection errors in pixels.

Method	Simulation	Real
Ours	1.3	1.8
ICP Initial Avg	21.1	115.1
ICP Initial Best	17.8	77.9
ICP Aligned Avg	2.8	5.2
ICP Aligned Best	2.5	5.5

Average pairwise root mean square reprojection errors in pixels.

Pair	Simulation	Real
LiDAR-RGB	2.6	3.1
Depth-RGB	3.4	4.0

Case Study 1

Comparative results

Average RGB-RGB root mean square reprojection errors in pixels.

Method	Simulation	Real
Ours	0.6	1.3
OpenCV	0.6	1.8
Kalibr	1.3	0.8

Average LiDAR-LiDAR root mean square reprojection errors in millimetres.

Method	Simulation	Real
Ours	33.0	53.6
ICP Initial Avg	249.4	173.4
ICP Initial Best	36.5	162.8
ICP Aligned Avg	33.9	53.3
ICP Aligned Best	91.7	109.9

Average LiDAR-depth root mean square reprojection errors in pixels.

Method	Simulation	Real
Ours	1.3	1.8
ICP Initial Avg	21.1	115.1
ICP Initial Best	17.8	77.9
ICP Aligned Avg	2.8	5.2
ICP Aligned Best	2.5	5.5

Average pairwise root mean square reprojection errors in pixels.

Pair	Simulation	Real
LiDAR-RGB	2.6	3.1
Depth-RGB	3.4	4.0

Case Study 1

Comparative results

Average RGB-RGB root mean square reprojection errors in pixels.

Method	Simulation	Real
Ours	0.6	1.3
OpenCV	0.6	1.8
Kalibr	1.3	0.8

Average LiDAR-LiDAR root mean square reprojection errors in millimetres.

Method	Simulation	Real
Ours	33.0	53.6
ICP Initial Avg	249.4	173.4
ICP Initial Best	36.5	162.8
ICP Aligned Avg	33.9	53.3
ICP Aligned Best	91.7	109.9

Average LiDAR-depth root mean square reprojection errors in pixels.

Method	Simulation	Real
Ours	1.3	1.8
ICP Initial Avg	21.1	115.1
ICP Initial Best	17.8	77.9
ICP Aligned Avg	2.8	5.2
ICP Aligned Best	2.5	5.5

Average pairwise root mean square reprojection errors in pixels.

Pair	Simulation	Real
LiDAR-RGB	2.6	3.1
Depth-RGB	3.4	4.0

Case Study 1

Comparative results

Average RGB-RGB root mean square reprojection errors in pixels.

Method	Simulation	Real
Ours	0.6	1.3
OpenCV	0.6	1.8
Kalibr	1.3	0.8

Average LiDAR-LiDAR root mean square reprojection errors in millimetres.

Method	Simulation	Real
Ours	33.0	53.6
ICP Initial Avg	249.4	173.4
ICP Initial Best	36.5	162.8
ICP Aligned Avg	33.9	53.3
ICP Aligned Best	91.7	109.9

Average LiDAR-depth root mean square reprojection errors in pixels.

Method	Simulation	Real
Ours	1.3	1.8
ICP Initial Avg	21.1	115.1
ICP Initial Best	17.8	77.9
ICP Aligned Avg	2.8	5.2
ICP Aligned Best	2.5	5.5

Average pairwise root mean square reprojection errors in pixels.

Pair	Simulation	Real
LiDAR-RGB	2.6	3.1
Depth-RGB	3.4	4.0

Case Study 1

Comparative results

Average RGB-RGB root mean square reprojection errors in pixels.

Method	Simulation	Real
Ours	0.6	1.3
OpenCV	0.6	1.8
Kalibr	1.3	0.8

Average LiDAR-LiDAR root mean square reprojection errors in millimetres.

Method	Simulation	Real
Ours	33.0	53.6
ICP Initial Avg	249.4	173.4
ICP Initial Best	36.5	162.8
ICP Aligned Avg	33.9	53.3
ICP Aligned Best	91.7	109.9

Average LiDAR-depth root mean square reprojection errors in pixels.

Method	Simulation	Real
Ours	1.3	1.8
ICP Initial Avg	21.1	115.1
ICP Initial Best	17.8	77.9
ICP Aligned Avg	2.8	5.2
ICP Aligned Best	2.5	5.5

Average pairwise root mean square reprojection errors in pixels.

Pair	Simulation	Real
LiDAR-RGB	2.6	3.1
Depth-RGB	3.4	4.0

Case Study 1

Comparative results

Average RGB-RGB root mean square reprojection errors in pixels.

Method	Simulation	Real
Ours	0.6	1.3
OpenCV	0.6	1.8
Kalibr	1.3	0.8

Average LiDAR-LiDAR root mean square reprojection errors in millimetres.

Method	Simulation	Real
Ours	33.0	53.6
ICP Initial Avg	249.4	173.4
ICP Initial Best	36.5	162.8
ICP Aligned Avg	33.9	53.3
ICP Aligned Best	91.7	109.9

Average LiDAR-depth root mean square reprojection errors in pixels.

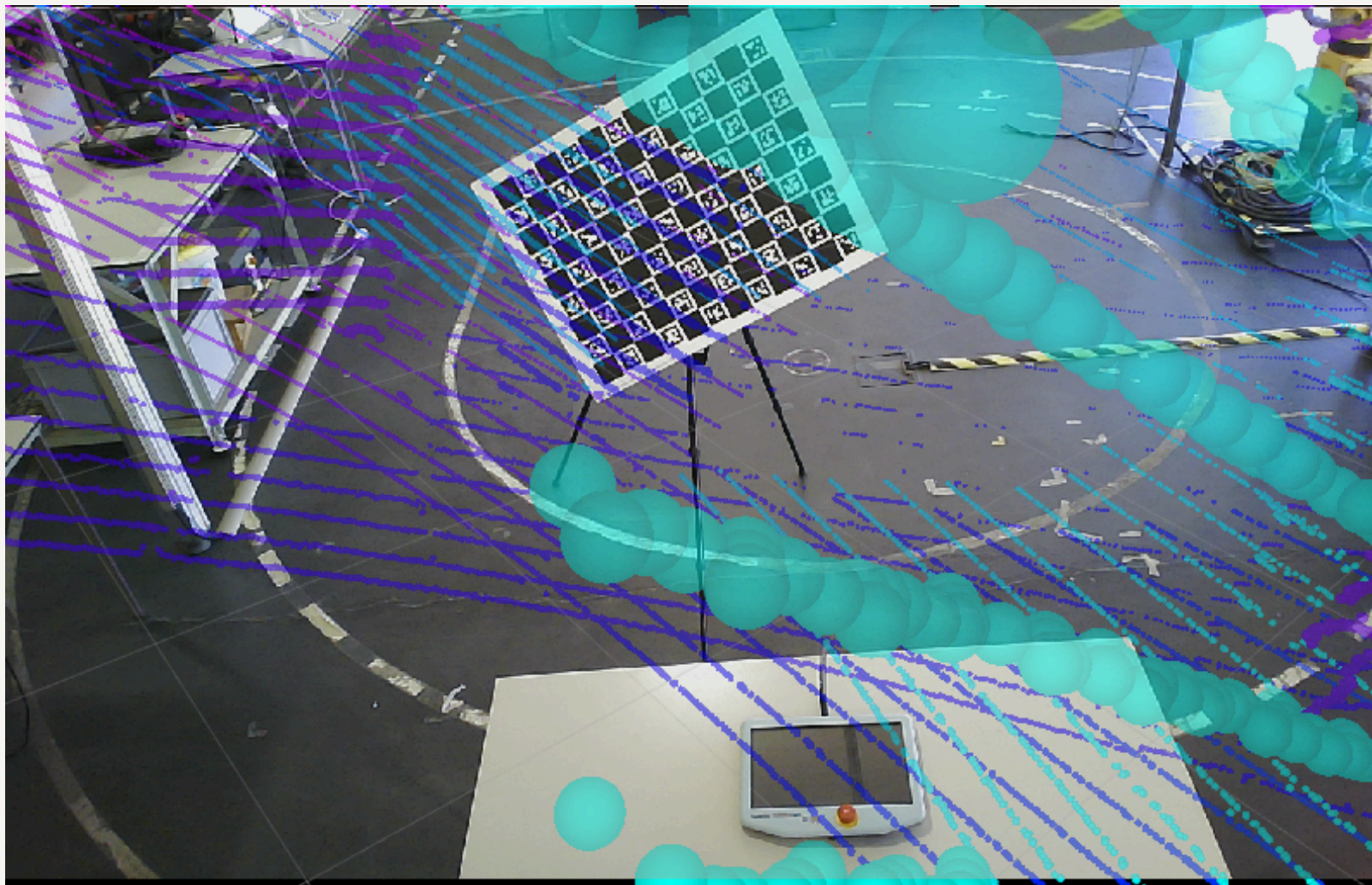
Method	Simulation	Real
Ours	1.3	1.8
ICP Initial Avg	21.1	115.1
ICP Initial Best	17.8	77.9
ICP Aligned Avg	2.8	5.2
ICP Aligned Best	2.5	5.5

Average pairwise root mean square reprojection errors in pixels.

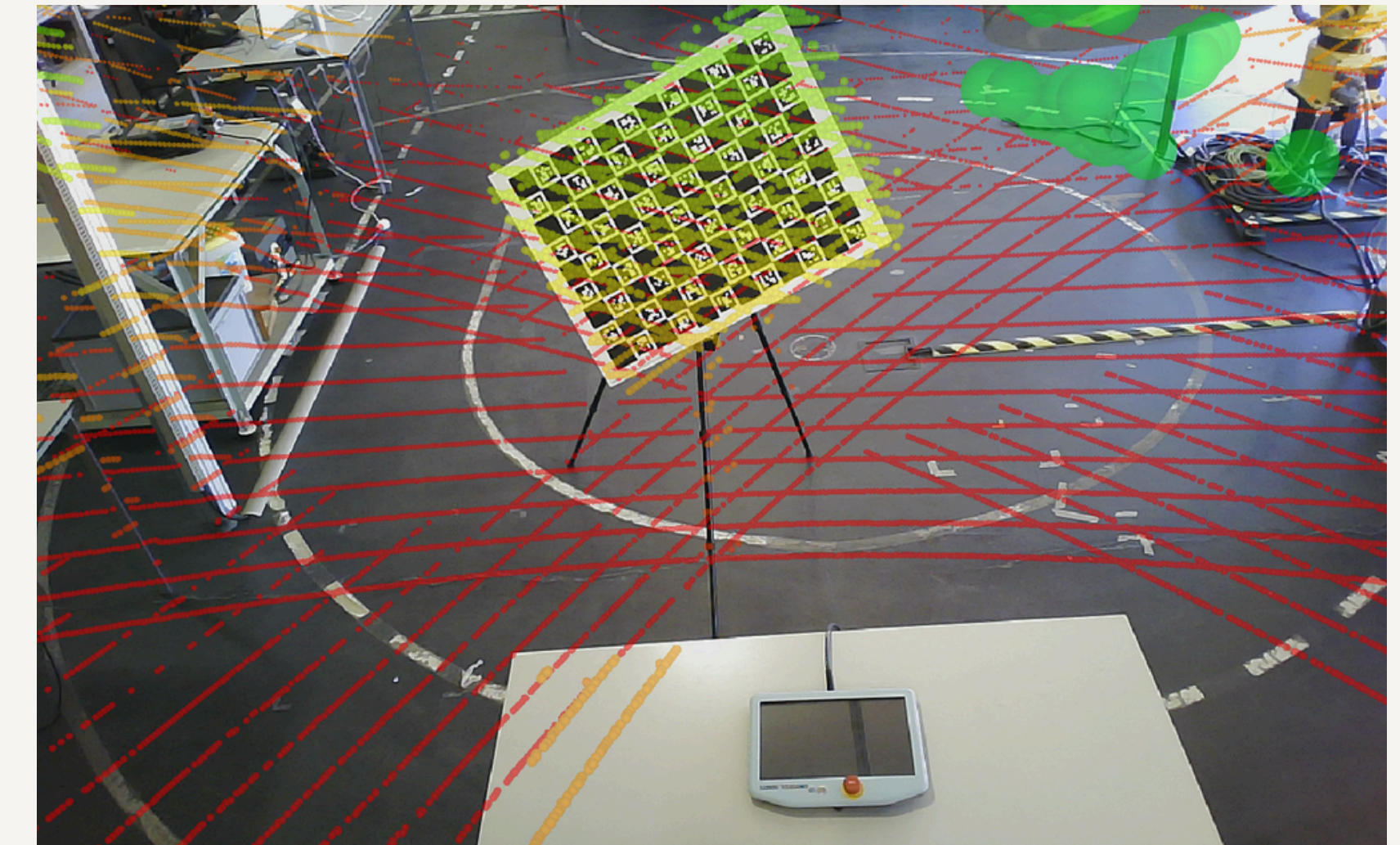
Pair	Simulation	Real
LiDAR-RGB	2.6	3.1
Depth-RGB	3.4	4.0

Case Study 1

Qualitative Results



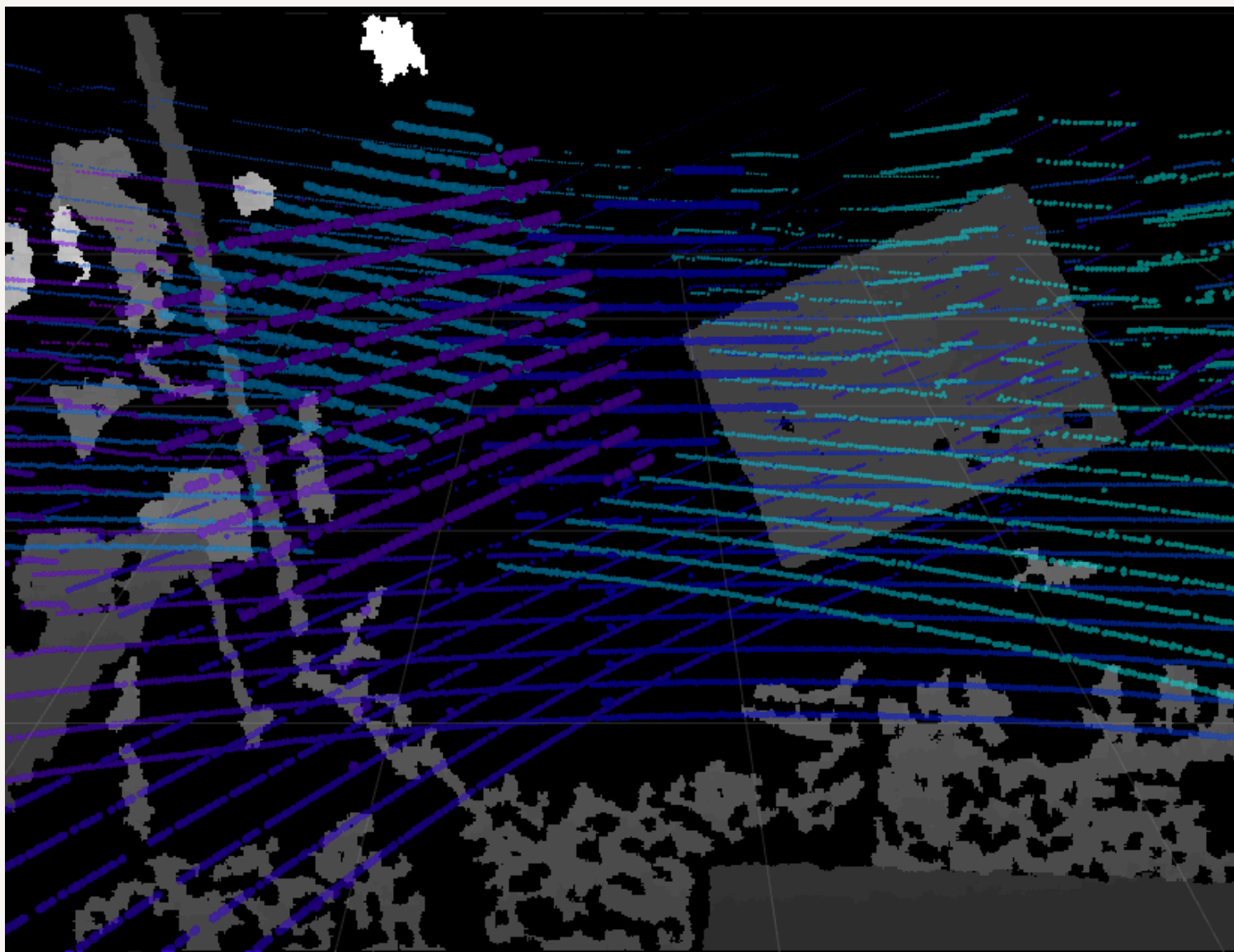
Projection of LiDAR's point clouds to an RGB image **before** calibration.



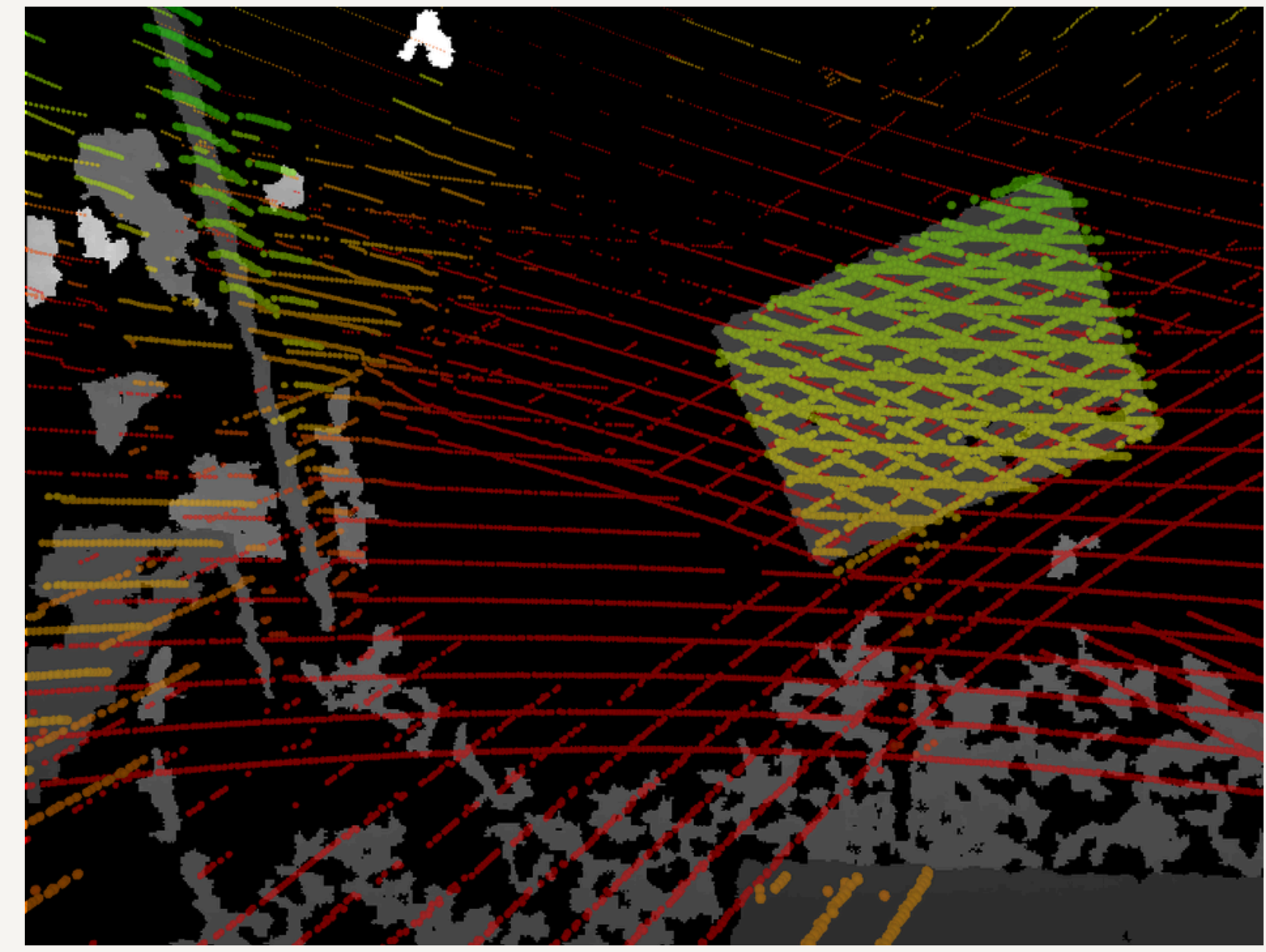
Projection of LiDAR's point clouds to an RGB image **after** calibration.

Case Study 1

Qualitative Results



Projection of LiDAR's point clouds to an RGB image **before** calibration..



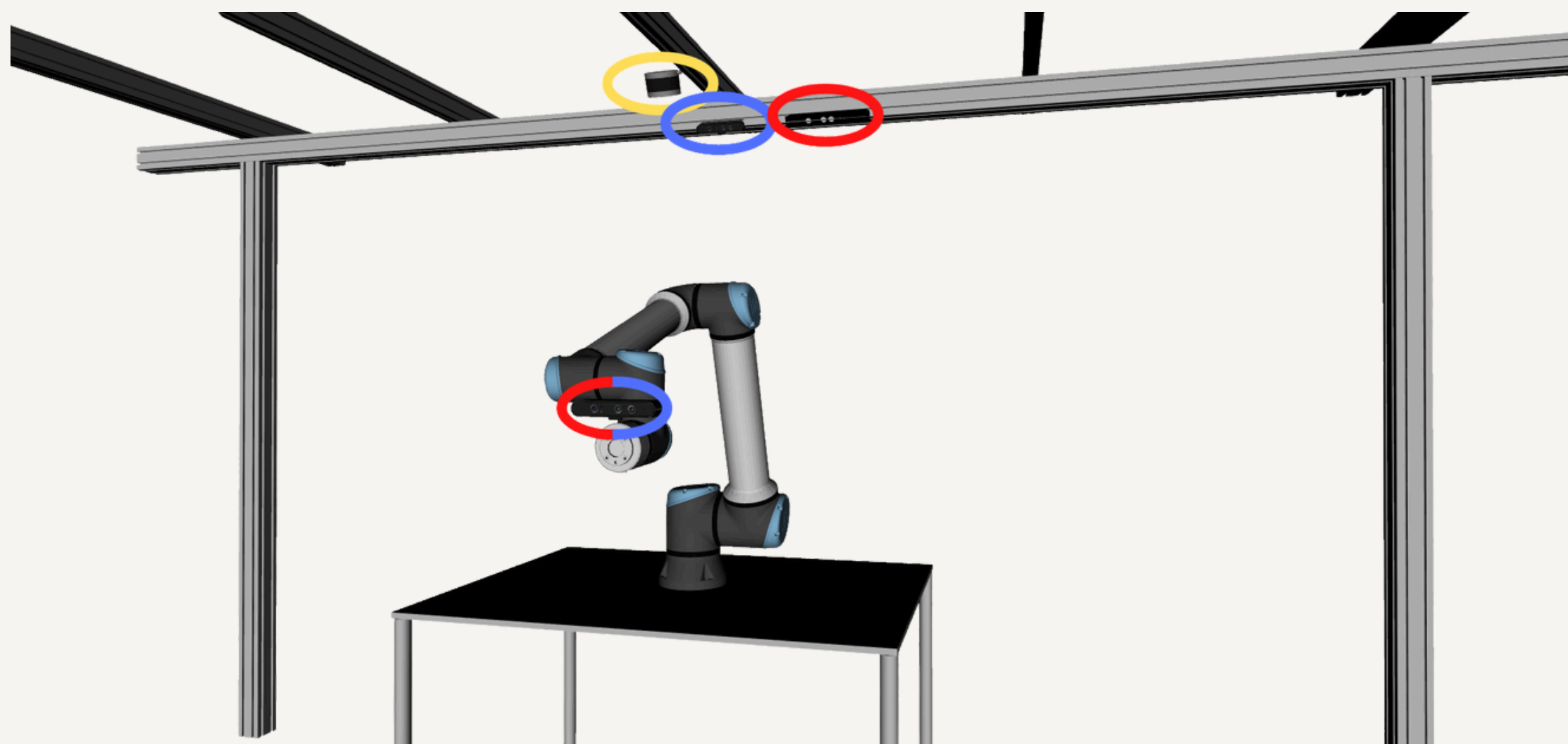
Projection of LiDAR's point clouds to an RGB image **after** calibration.

Case Study 2

Experiment definition

Descriptions of the datasets used in this experiment.

Type of data	Dataset	# collections	# partials	# complete
Simulation	train dataset	22	4	22
	test dataset	10	2	9
Real data	train dataset	29	58	11
	test dataset	13	26	5



Red - Depth; Yellow - LiDAR; Blue - RGB

Sensors

- 1 LiDAR
- 1 RGB-D (hand-eye)
- 1 RGB
- 1 Depth

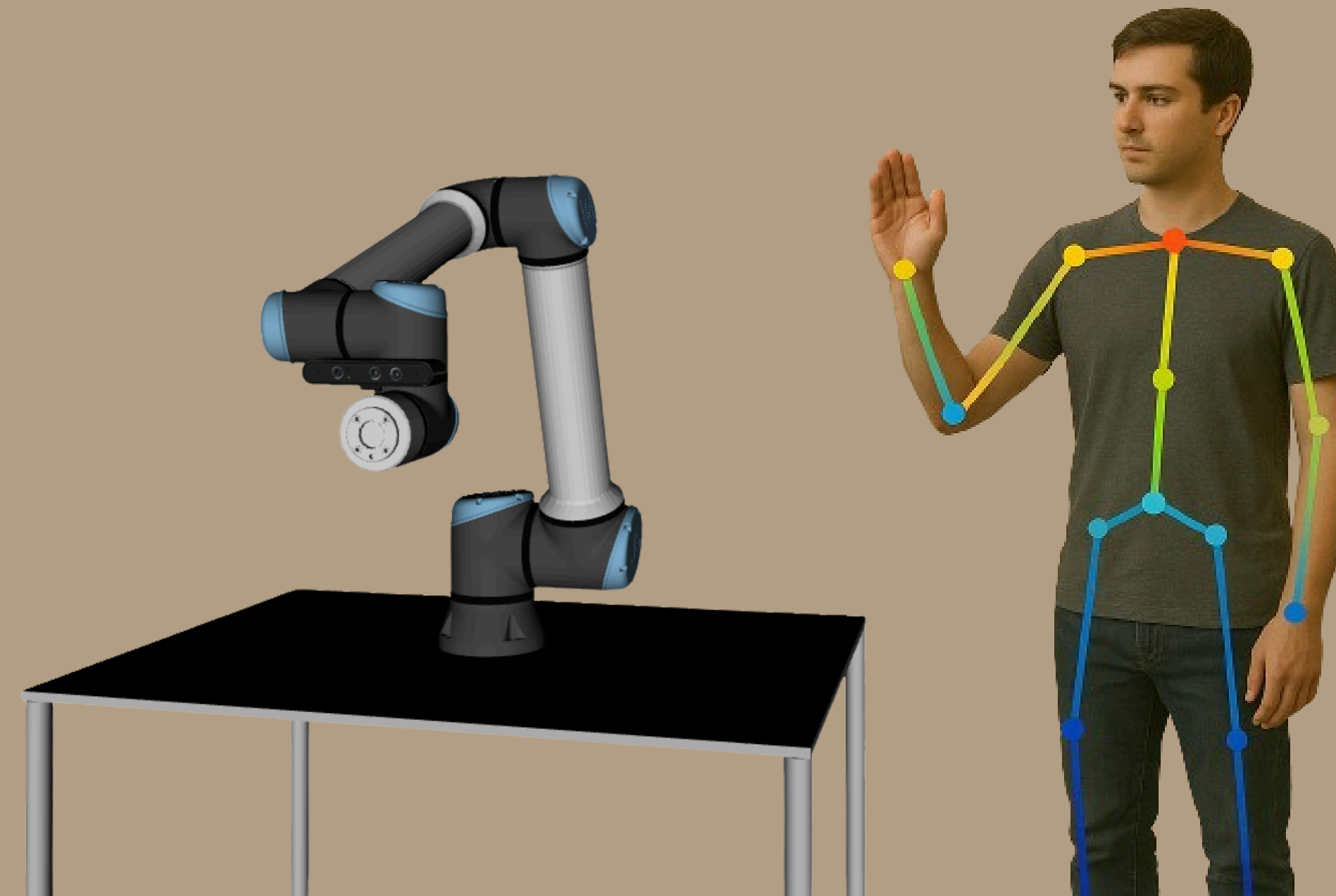
Case Study 2

Quantitative Results

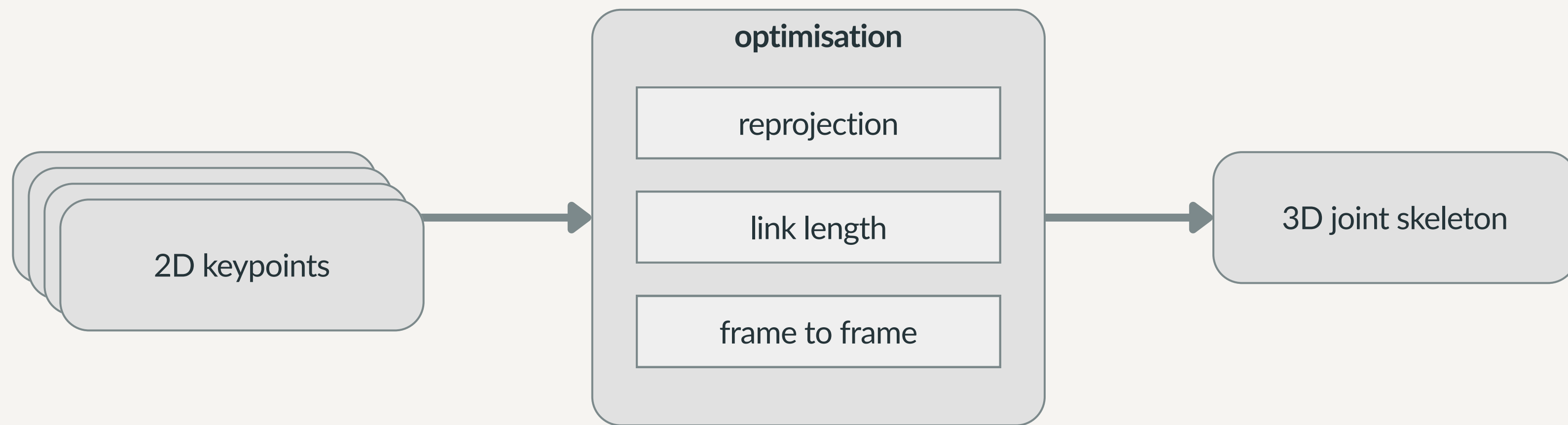
Average pairwise reprojection errors in pixels.

Pair	Simulation	Real
RGB-RGB	0.7	3.7
LiDAR-RGB	1.9	5.5
LiDAR-Depth	1.9	4.7
Depth-RGB	1.9	4.6
Depth-Depth	1.5	3.6

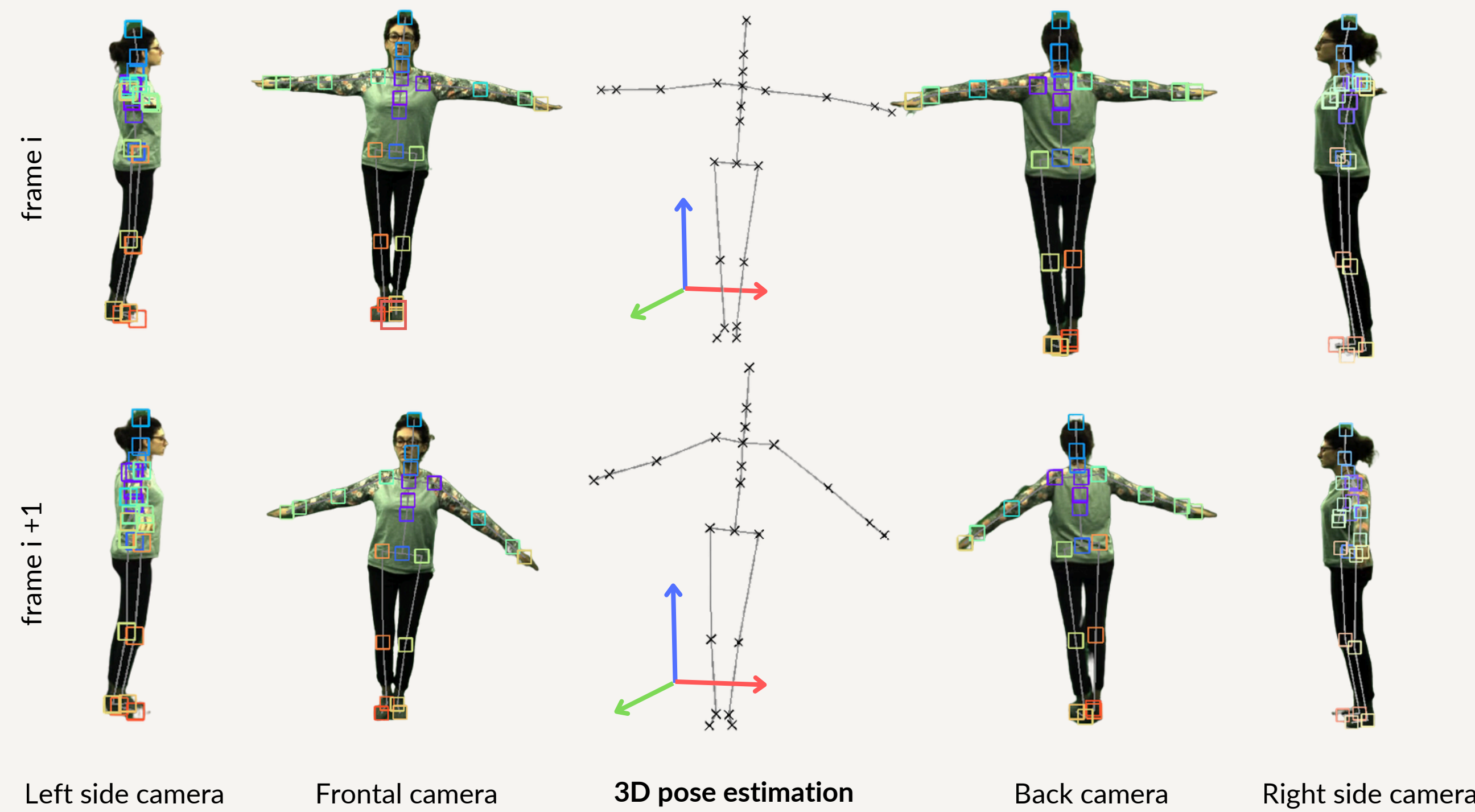
Human Pose Estimation



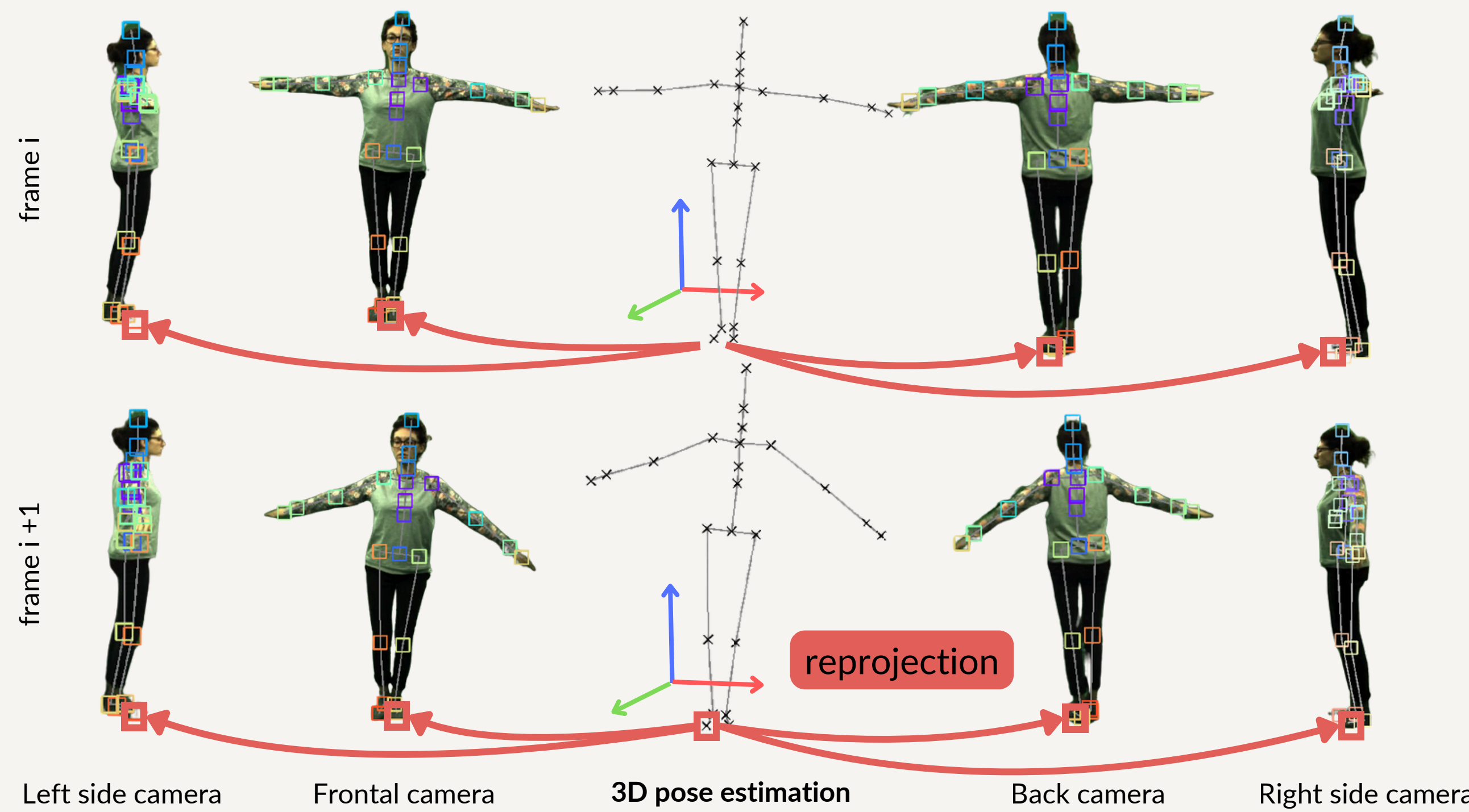
3D Human Pose Estimation Pipeline



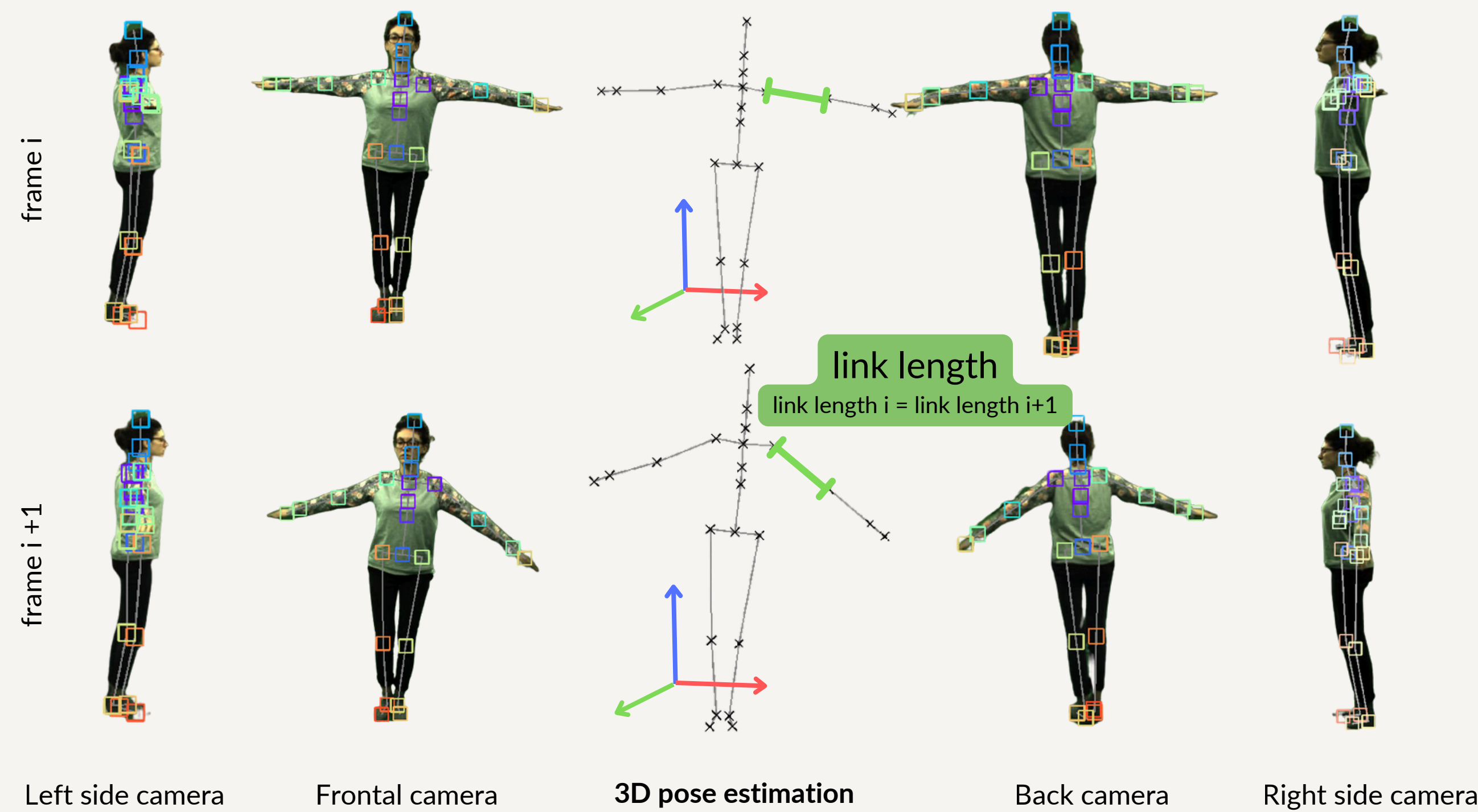
3D Human Pose Estimation



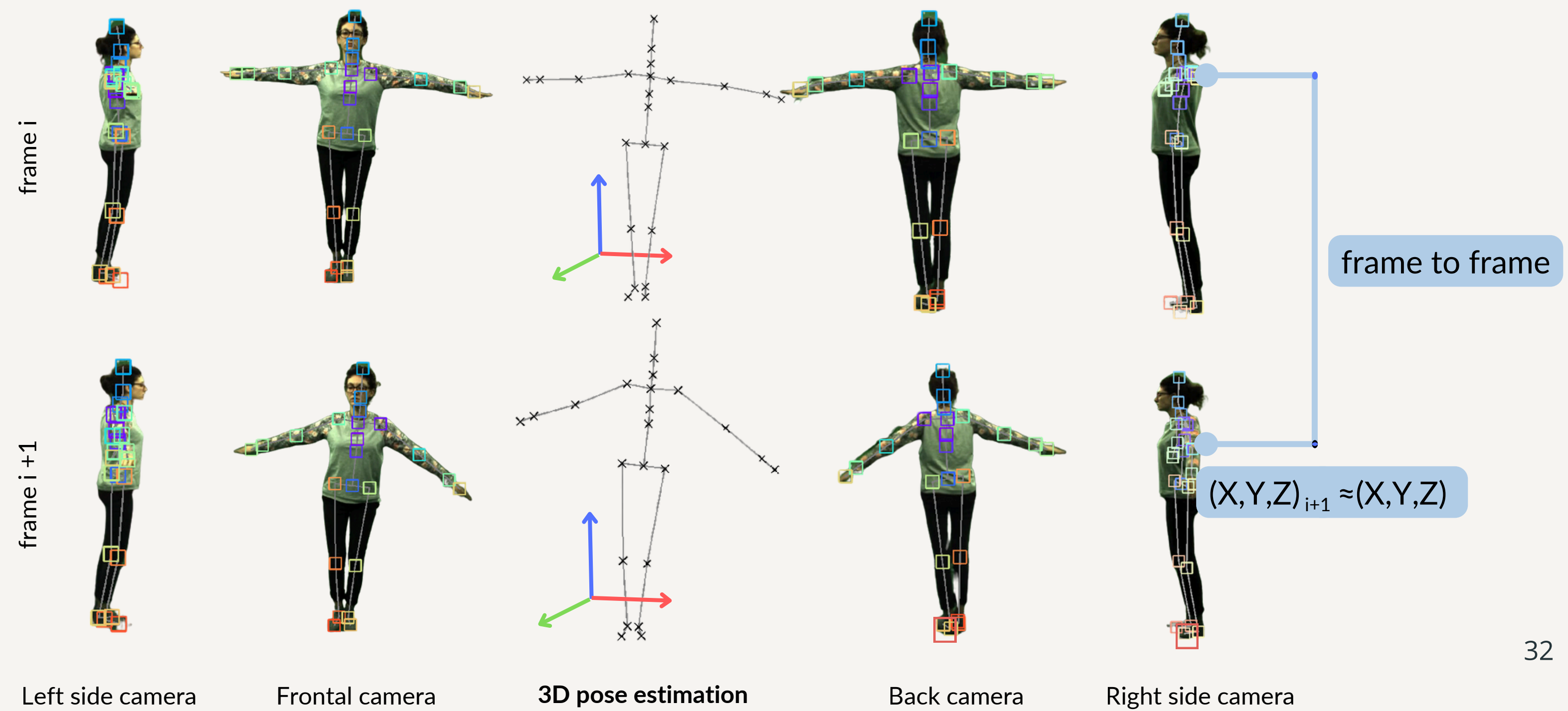
3D Human Pose Estimation



3D Human Pose Estimation



3D Human Pose Estimation



3D Human Pose Estimation

Objective Function

$$f_{obj} = \arg \min_{(X,Y,Z)_{i,f}} \sum_j e_{ll} + \sum_i \sum_f (e_{rp} - e_{ff})$$

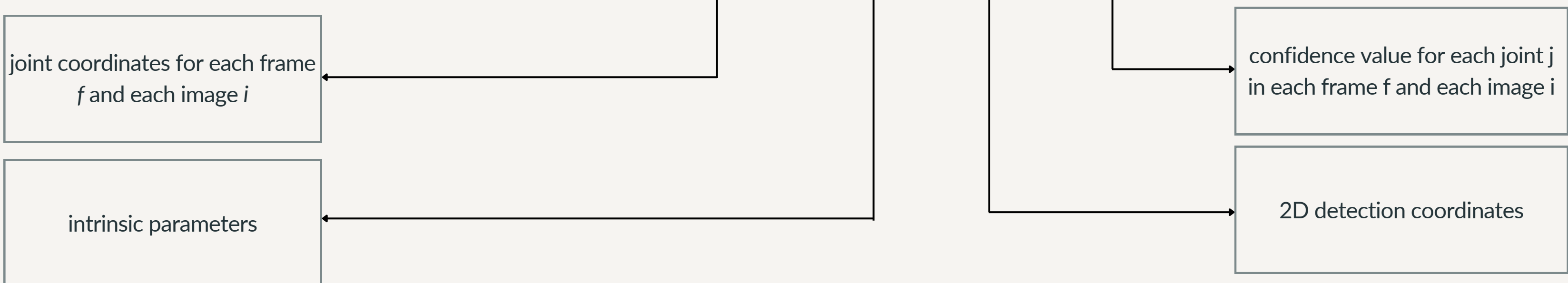
3D Human Pose Estimation

Objective Function

$$f_{obj} = \arg \min_{(X,Y,Z)_{i,f}} \sum_j e_{ll} + \sum_i \sum_f (e_{rp} - e_{ff})$$

Reprojection Error

$$e_{rp} = \left\| proj \left((X, Y, Z)_{i,f}, \lambda_i \right) - d_{j,f,i} \right\| \cdot c_{j,f,i}$$



3D Human Pose Estimation

Objective Function

$$f_{obj} = \arg \min_{(X,Y,Z)_{i,f}} \sum_j e_{ll} + \sum_i \sum_f (e_{rp} + e_{ff})$$

3D Human Pose Estimation

Objective Function

$$f_{obj} = \arg \min_{(X,Y,Z)_{i,f}} \sum_j e_{ll} + \sum_i \sum_f (e_{rp} + e_{ff})$$

Link length Error

$$e_{ll} = \sqrt{\frac{\sum_f (l_{j,f} - \bar{l}_j)^2}{F}}$$

link length for joint j and frame f

average link length for joint j

total number of frames

3D Human Pose Estimation

Objective Function

$$f_{obj} = \arg \min_{(X,Y,Z)_{i,f}} \sum_j e_{ll} + \sum_i \sum_f (e_{rp} + e_{ff})$$

3D Human Pose Estimation

Objective Function

$$f_{obj} = \arg \min_{(X, Y, Z)_{i,f}} \sum_j e_{ll} + \sum_i \sum_f (e_{rp} + e_{ff})$$

Frame-to-frame Error

$$e_{ff} = \begin{cases} \|(X, Y, Z)_{i,f} - (X, Y, Z)_{j,f-1}\|, & \text{if } j \text{ occluded} \\ 0, & \text{otherwise} \end{cases}$$

joint coordinates for frame f
and each image i

joint coordinates for frame $f-1$
and each image i

Quantitative Results

Results reported by other state-of-the-art 2D to 3D lifting approaches.

Experiment Details

Dataset: MPI-INF-3DHP

Skeleton: 23 joints

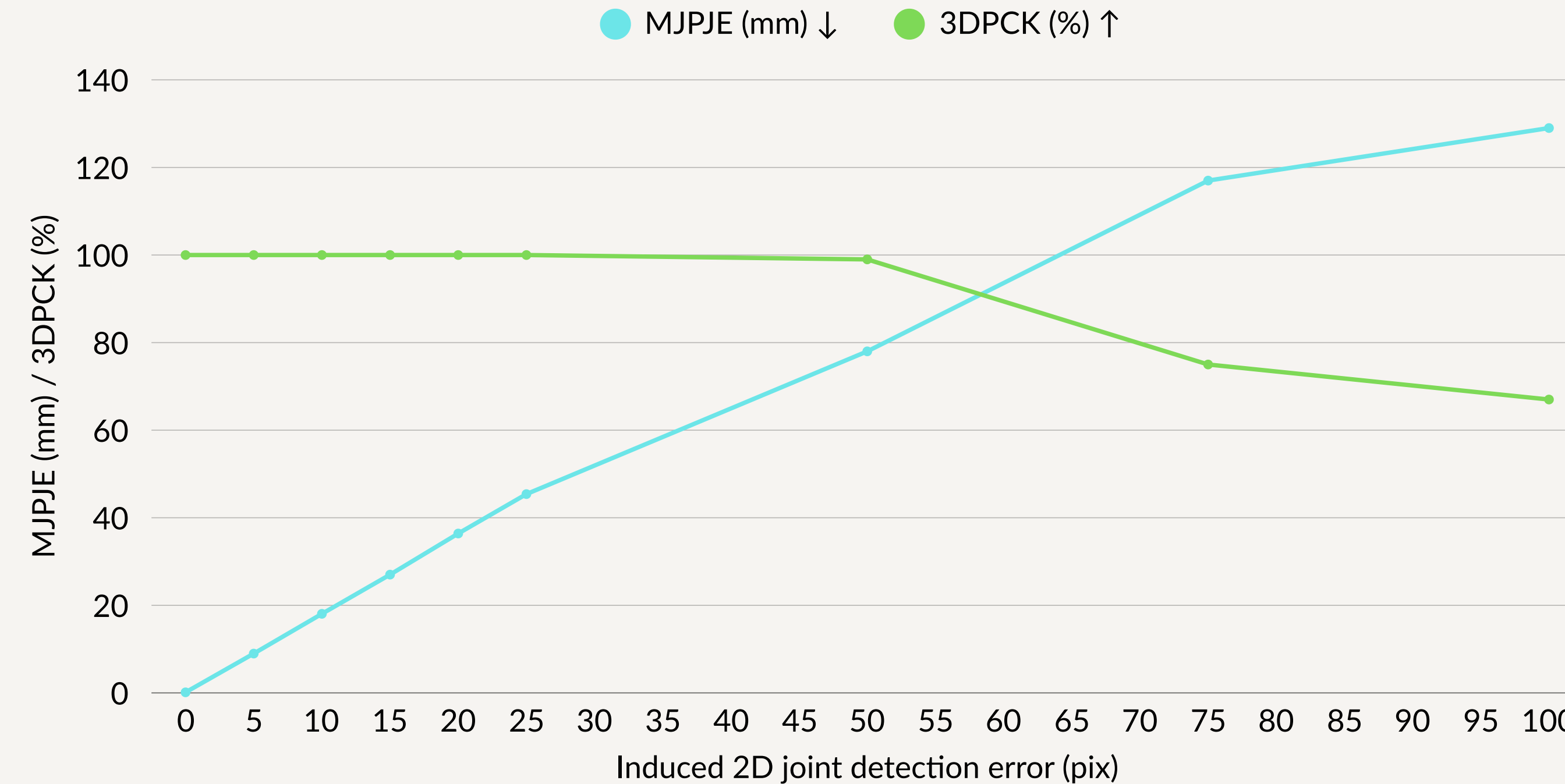
Cameras: 4

Methodology	MPJPE (mm) ↓
Kocabas et al. (CVPR 2019)	109.0
Bouazizi et al. (AVSS 2021)	93.0
Pavvlo et al. (CVPR 2019)	86.6
Bouazizi et al. (FG 2021)	65.9
Jiang et al. (WACV 2024)	55.2
Zhao et al. (CVPR 2023)	27.8
Yu et al. (CVPR 2023)	27.8
Ours (20px error)	36.4
Ours (10px error)	18.1

Mean Per Joint Position Error (MPJPE) in millimeters.

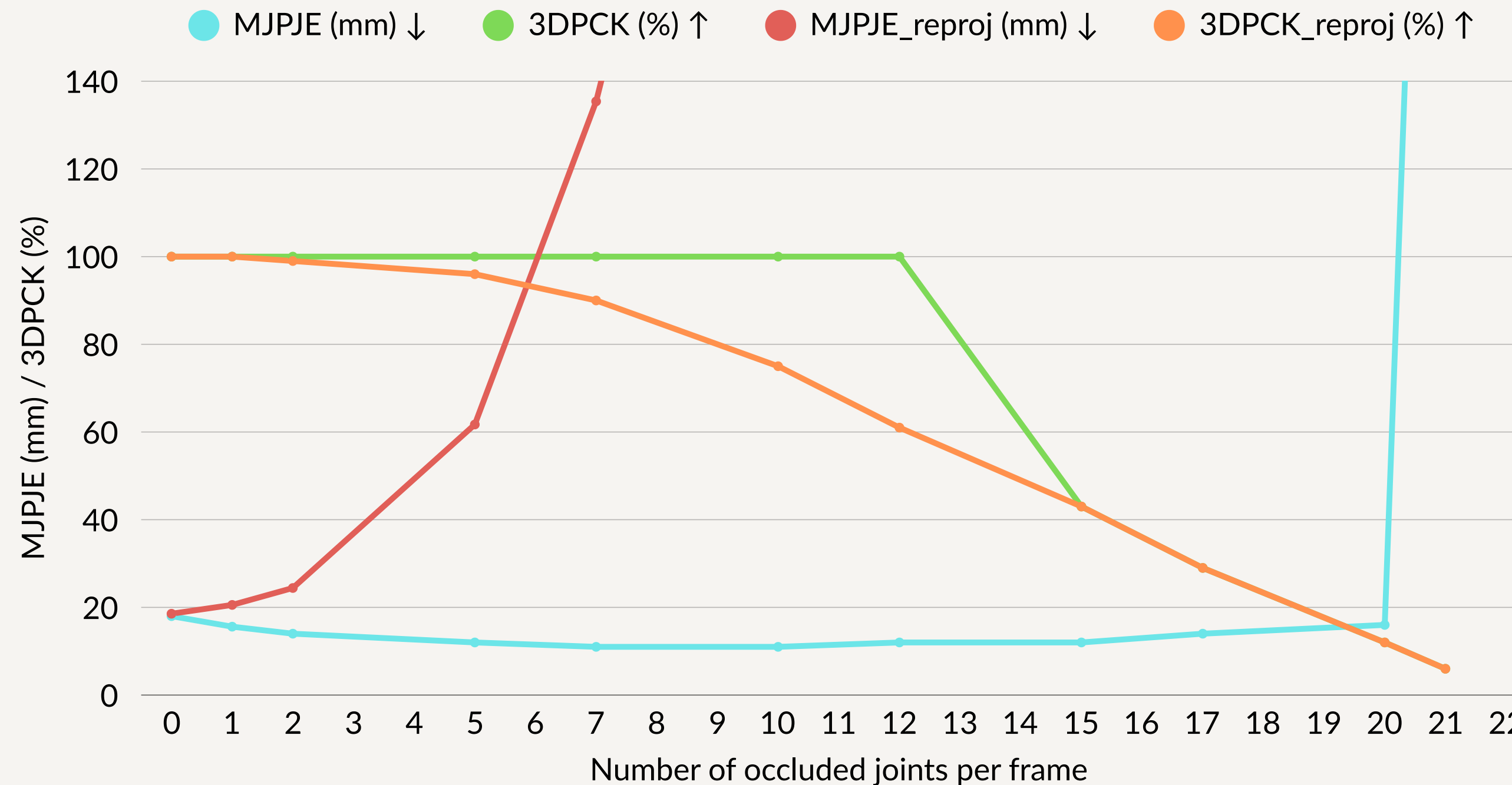
Quantitative Results

Impact of 2D joint detection error in detection of human 3D poses



Quantitative Results

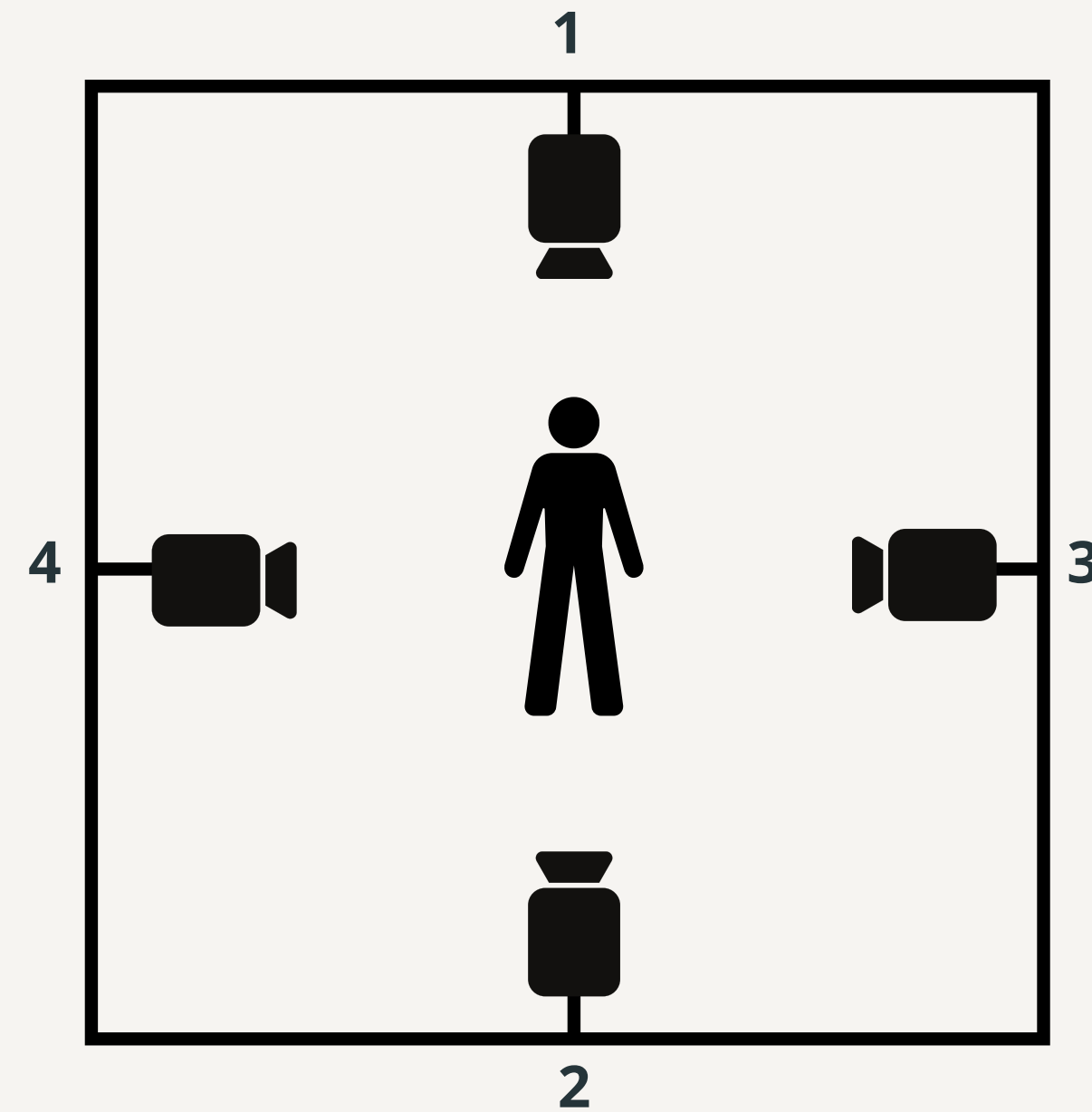
Impact of occluded 2D joints in the detection of human 3D poses



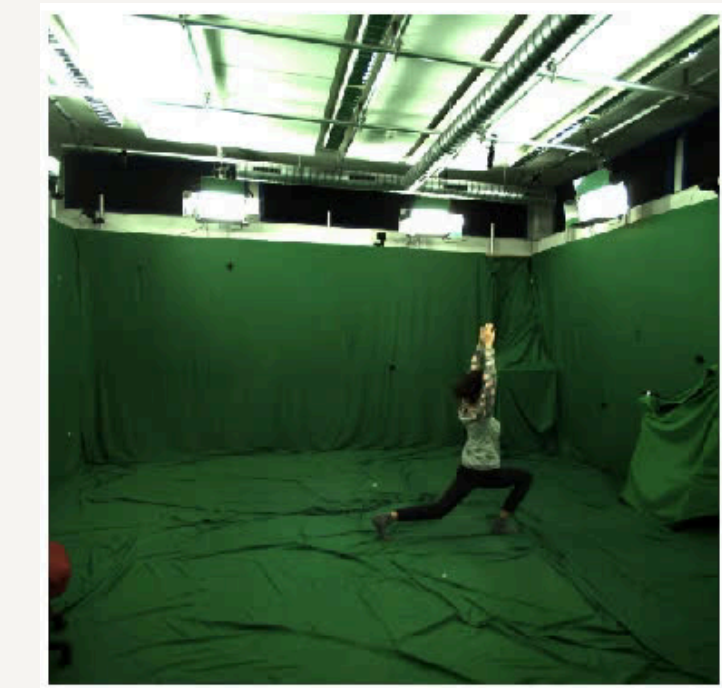
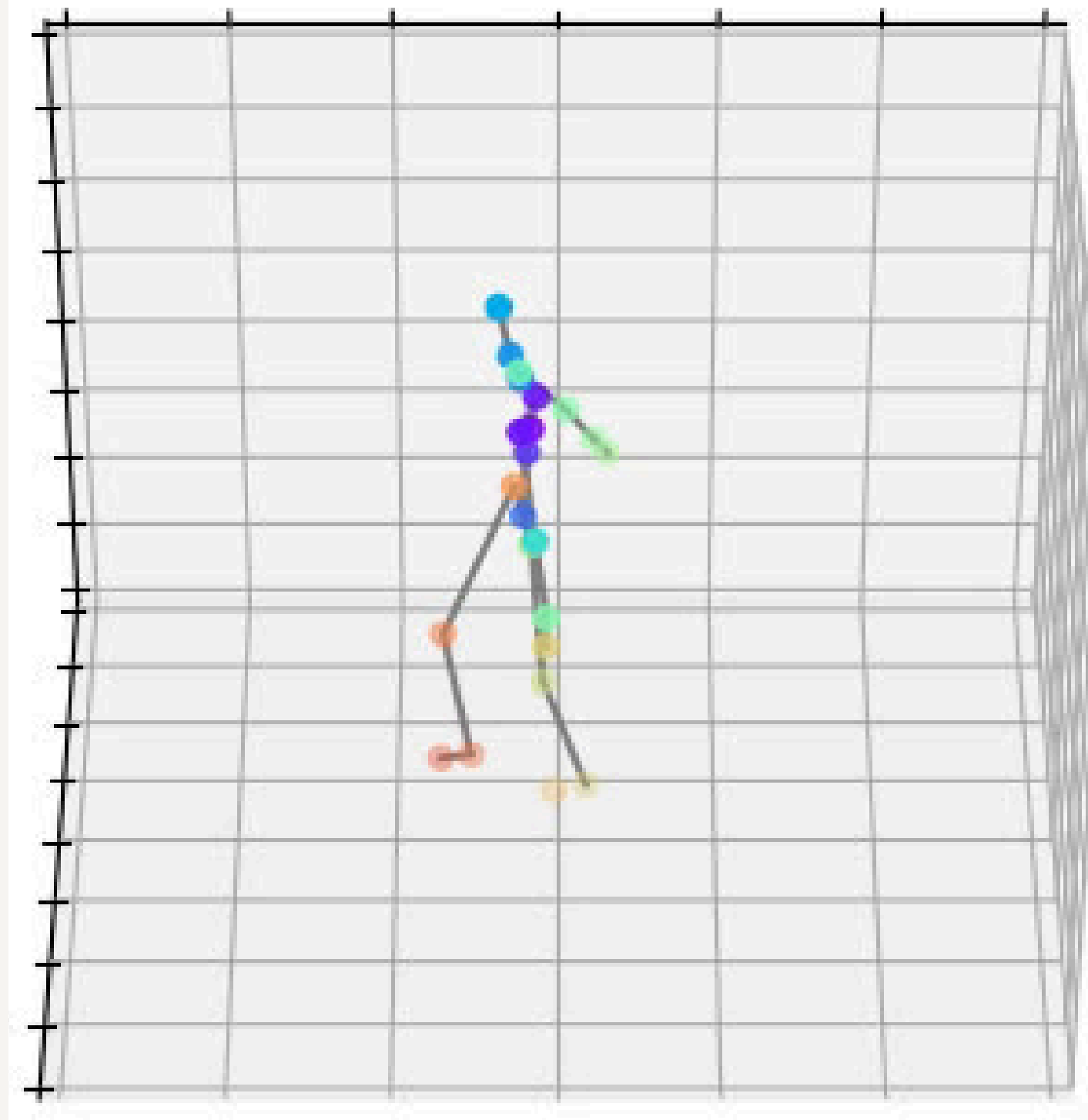
Quantitative Results

Impact of the number of cameras in the MPJPE (mm) and 3DPCK (%).

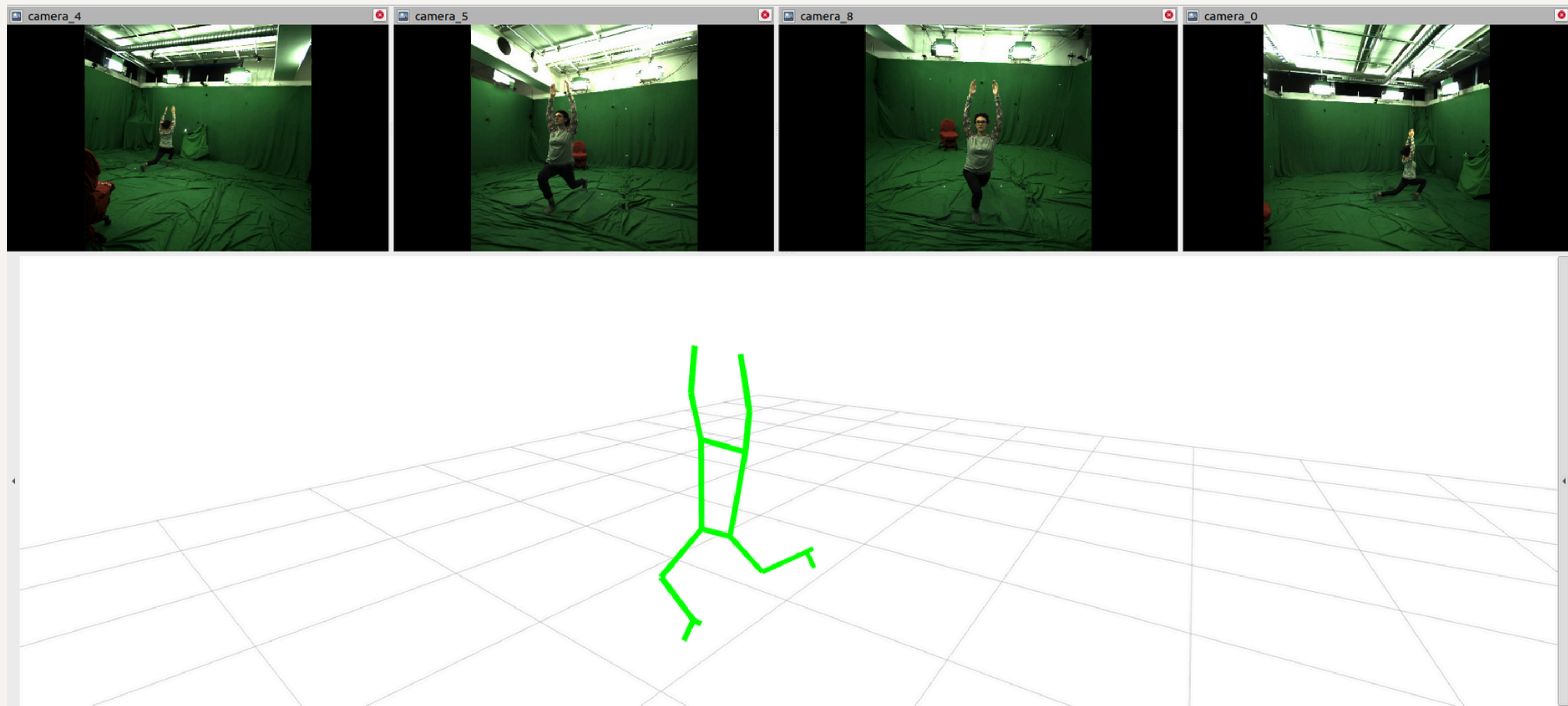
# cameras	MPJPE	3DPCK
2	47.4	96.2
3	13.8	100
4	11.6	100



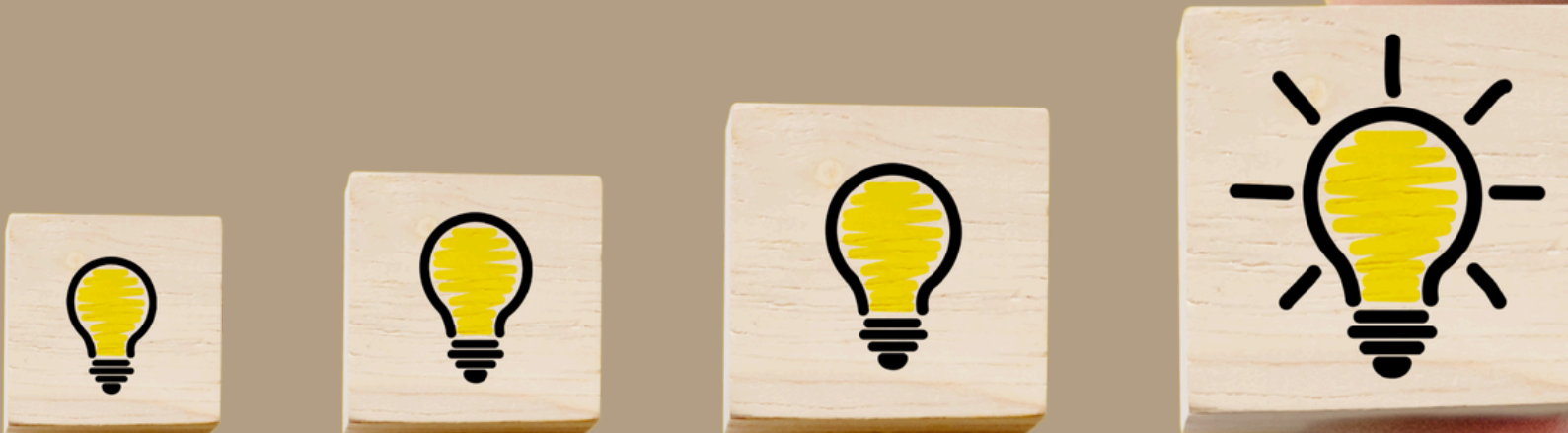
Qualitative Results



ROS Integration



Conclusions and Future Work



Contributions and Implications

Contributions

- Extended ATOM framework to support **RGB-D** cameras, including **hand-eye calibration**.
- Rigorous testing in simulated and real robotic setups, achieving **accuracy and robustness under motion**.
- Multi-camera RGB pipeline for **3D human pose estimation** in collaborative workspaces.
- Open-source implementation and integration in ROS, adaptable to **industrial collaborative cells**.

Contributions and Implications

Contributions

- Extended ATOM framework to support **RGB-D** cameras, including **hand-eye calibration**.
- Rigorous testing in simulated and real robotic setups, achieving **accuracy and robustness under motion**.
- Multi-camera RGB pipeline for **3D human pose estimation** in collaborative workspaces.
- Open-source implementation and integration in ROS, adaptable to **industrial collaborative cells**.

Implications

Scientific: Bridges two core **perception** challenges (calibration and pose estimation) in **one framework**.

Practical: Supports **safer**, more **flexible**, and **human-aware** robot collaboration.

Thesis Publications

- Rato D., Oliveira M., Santos V., Gomes M., Sappa A. (2022), A sensor-to-pattern calibration framework for multi-modal industrial collaborative cells. In: **Journal of Manufacturing Systems**, doi: [10.1016/j.jmsy.2022.07.006](https://doi.org/10.1016/j.jmsy.2022.07.006)
- Rato D., Oliveira M., Santos V., Sappa A., Raducanu B. (2024), Multi-View 2D to 3D Lifting Video-Based Optimization: A Robust Approach for Human Pose Estimation with Occluded Joint Prediction. In: 2024 IEEE/RSJ International Conference on Intelligent Robots and Systems (**IROS 2024**), doi: [10.1109/IROS58592.2024.10802200](https://doi.org/10.1109/IROS58592.2024.10802200)
- Rato D., Oliveira M., Santos V., Sappa A., New Methodology to Calibrate Depth Sensors in Multi-Modal Dynamic Setups. Submitted: **IEEE Access**

Conclusions and Future Work

Conclusions

- Robust calibration in complex robotic systems is feasible with the extended ATOM framework.
- Multi-camera RGB pose estimation significantly improves **accuracy and robustness under occlusion**.
- Both are essential building blocks for **perception-driven human-robot collaboration**.

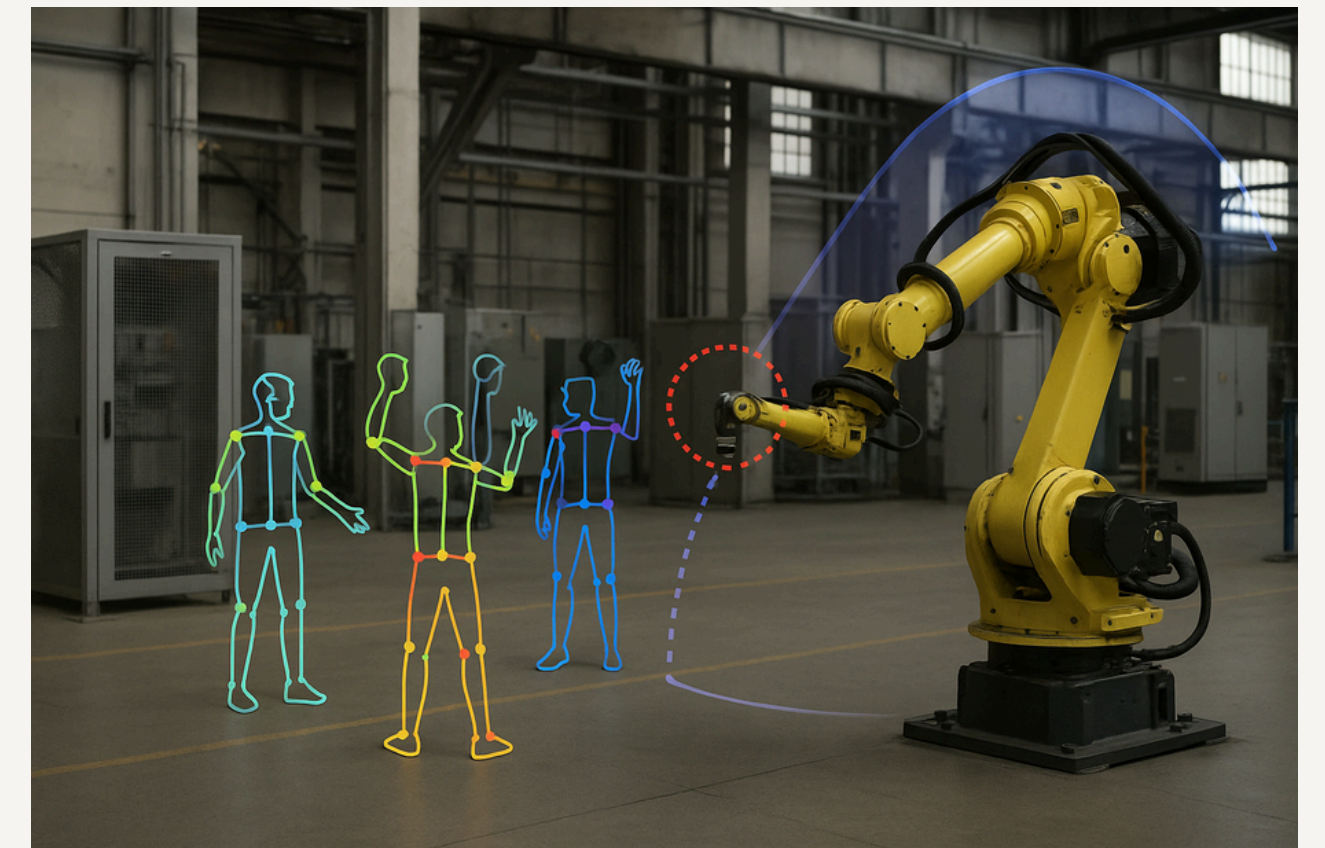
Conclusions and Future Work

Conclusions

- Robust calibration in complex robotic systems is feasible with the extended ATOM framework.
- Multi-camera RGB pose estimation significantly improves accuracy and robustness under occlusion.
- Both are essential building blocks for perception-driven human–robot collaboration.

Future Work

- Online / adaptive calibration for dynamic setups.
- Multi-person pose estimation with temporal consistency.
- Integration with robot control for predictive and safety-aware behaviour.
- Industrial benchmarking under diverse, real-world conditions.



Thank You

The author acknowledges the support of the Project Augmented Humanity [POCI-01-0247-FEDER-046103] and the CYTED Network: Ibero-American Thematic Network on ICT Applications for Smart Cities (RF-518RT0559).

This work was supported by FCT - Fundação para a Ciência e Tecnologia, I.P. by project reference 2021.04792.BD and DOI identifier <https://doi.org/10.54499/2021.04792.BD>.



UNIÃO EUROPEIA
Fundo Social Europeu

